L'Institut Agro Rennes-Angers
Site de Rennes

Année universitaire : 2024 - 2025 Spécialité : Sciences halieutiques et aquacoles Spécialisation (et option éventuelle) : « Statistiques et modélisation »	**Mémoire de fin d'études** d'ingénieur de l'Institut Agro Rennes-Angers (Institut national d'enseignement supérieur pour l'agriculture, l'alimentation et l'environnement)

High-Resolution Projections of South Pacific Sea Surface Temperature through Statistical Downscaling and Bias Correction

Par : Lou BEATA

Soutenu à Rennes le 10/09/2025

Devant le jury composé de :

Président : Etienne RIVOT

Maître de stage : Ricardo OLIVEROS-RAMOS

Enseignant référent : Etienne RIVOT

Autres membres du jury (Nom, Qualité)

Olivier LE PAPE (Enseignant-chercheur L'institut Agro Rennes-Angers)

Hubert DU PONTAVICE (Chargé de recherche)

Acknowledgements :

I would like to express my deepest gratitude to all those who contributed to the completion of this Master's report.

First and foremost, I am especially grateful to my supervisor, Ricardo Oliveros-Ramos, for his guidance, advice, and encouragement throughout this internship. His constant support, constructive feedback, and scientific insight greatly shaped the direction of this project and ensured that I was able to make the most of this experience.

I would also like to warmly thank Yunne-Jai Shin for welcoming me to MARBEC and for giving me the opportunity to carry out this project within her team. Her valuable advice, scientific perspective, and thoughtful encouragements were instrumental throughout the entire course of my work.

I am also very grateful to my academic tutor, Mr. Rivot, who showed interest in my project from the very beginning and provided guidance in the writing of this report. I would also like to extend my thanks to all the professors at Institut Agro Rennes, who provided us with strong knowledge and skills throughout the course of our engineering studies, which served as a foundation for this work.

I am particularly thankful to the members of the SPRFMO for supporting this project and allowing it to come to life, creating an opportunity to link research directly with fisheries management issues.

My thanks also go to my colleagues at MARBEC for welcoming me warmly during my six months in the research unit and for the stimulating discussions, insightful presentations, and friendly environment that made this internship both productive and enjoyable.

Finally, I wish to thank all those who, directly or indirectly, contributed to the completion of this report. Whether through enriching discussions, constructive advice, or simply their presence, their support has been truly meaningful.

This report is the result of both collective and personal effort, and I am deeply grateful to everyone who accompanied me along the way.

Table of Contents

Glossary

- **Sea Surface Temperature (SST) / Température de surface de la mer (SST)** : température mesurée à la surface des océans, variable clé du climat et des écosystèmes marins.
- **Earth System Model (ESM) / Modèle du système Terre (ESM)** : modèle numérique intégrant atmosphère, océan, glace et biosphère pour simuler le climat global.
- **CMIP (Coupled Model Intercomparison Project)** : initiative internationale qui coordonne les expériences de modélisation du climat afin de comparer et améliorer les modèles.
- **RCP (Representative Concentration Pathway)** : scénarios de concentration de gaz à effet de serre utilisés dans le CMIP5, décrivant des trajectoires possibles du forçage radiatif.
- **SSP (Shared Socioeconomic Pathway)** : scénarios socio-économiques développés pour le CMIP6, combinés avec les RCP pour explorer les futurs climatiques possibles.
- **Bias correction / Correction de biais** : méthode statistique visant à corriger les écarts systématiques entre les sorties de modèles climatiques et les observations.
- **Downscaling / Descente d'échelle** : techniques (statistiques ou dynamiques) permettant de passer de projections climatiques globales à des résolutions régionales/locales plus fines.
- **ENSO (El Niño–Southern Oscillation) / Oscillation australe El Niño** : phénomène climatique majeur du Pacifique tropical qui influence la température, les précipitations et les écosystèmes mondiaux.
- **Quantile mapping / Cartographie de quantiles** : technique de correction de biais consistant à ajuster la distribution statistique d'une variable simulée pour qu'elle corresponde à celle observée.
- **Overshoot scenario / Scénario de dépassement** : scénario climatique où la température dépasse temporairement un seuil (ex. +2 °C) avant de redescendre grâce à des réductions fortes d'émissions ou à des techniques d'élimination du carbone.
-

List of abbreviations

SST : Sea Surface Temperature
ESM : Earth System Model
CMIP : Coupled Model Intercomparison Project
RCP : Representative Concentration Pathway
SSP : Shared Socioeconomic Pathway
OISST : Optimum Interpolation Sea Surface Temperature
GAM : Generalized Additive Model / Modèle additif généralisé
ENSO : El Niño–Southern Oscillation
MAE : Mean Absolute Error
CTE : Conditional Tail Expectation
RAM : Random Access Memory

List of Figures and Tables

List of Appendices

Introduction

Climate change is one of the most pressing global challenges, with widespread impacts on both environmental and socio-economic systems. It drives rising temperatures, more frequent extreme events, sea level rise, and ocean acidification, all of which pose significant risks to ecosystems and human societies (Guinotte, Fabry, 2008; Christensen *et al.*, 2011; Calvin *et al.*, 2023). Among the drivers of interannual variability, the El Niño–Southern Oscillation (ENSO) is particularly influential in the Pacific, shaping ocean temperature, precipitation, and ecosystem dynamics (Brown et al., 2020).

In the South Pacific, these pressures directly affect marine-based economies, especially fisheries, which are vital for food security, livelihoods, and export income across island nations. Climate-driven increases in sea surface temperature (SST) can push species beyond their thermal limits, disrupt life-history processes, and trigger local stock declines or collapses with cascading socio-economic consequences (Hastings *et al.*, 2020; Vogel *et al.*, 2023; Xu *et al.*, 2024). At the same time, warming waters drive poleward shifts in distribution, potentially moving valuable resources across jurisdictional boundaries or into international waters, complicating access rights and management frameworks. This vulnerability is amplified for small island communities highly dependent on climate-sensitive sectors such as fisheries, tourism, and coastal resources (Pacific Community Results Report, 2023). Anticipating where and when such shifts will occur requires reliable, spatially explicit climate projections that can support adaptive strategies, whether through adjusting quotas, relocating fishing effort, or redesigning management boundaries (Heenan *et al.*, 2015).

While Earth System Models (ESMs) provide valuable large-scale climate projections, their typical resolution (around 1° or 100 km) is too coarse to resolve the fine-scale features critical in island-rich and topographically complex regions (Xu *et al.*, 2019; Kristiansen *et al.*, 2024). Moreover, raw ESM outputs often exhibit systematic biases due to limitations in physical representations, which reduces their reliability for localized climate assessments (Cannon *et al.*, 2020; Pozo Buil *et al.*, 2023). These coarse and biased outputs are often insufficient for impact models that require local accuracy, especially in narrow shelf zones or nearshore environments (Drenkard *et al.*, 2021). A way to make these outputs more reliable and useful at the regional scale is through downscaling, the process of translating coarse-resolution climate information into finer-scale projections. Two main approaches exist: dynamical downscaling, which uses regional climate models but is computationally expensive and still subject to biases, and statistical downscaling, which builds empirical relationships between large-scale model outputs and local observations. Statistical downscaling is computationally efficient and allows the production of high-resolution, bias-corrected projections, but it relies on the assumption that the statistical relationships established from the past and present remain valid in the future (Fowler *et al.*, 2007; Ahmed *et al.*, 2013; Oliveros-Ramos *et al.*, 2025). By refining ESM outputs in this way, statistical downscaling produces climate inputs that are both realistic and ecologically relevant, where even a 1 °C bias can critically alter predictions of species distributions or ecosystem stress.

However, most downscaling studies have focused on continental regions, with only limited efforts addressing the unique climatic and geographic characteristics of the South Pacific, a region dominated by small islands and complex land–ocean interactions (Kristiansen *et al.*, 2024). Despite the ecological importance of the tropical Pacific, downscaled marine datasets remain scarce and fragmented (Ruti *et al.*, 2016; Drenkard *et al.*, 2021). This persistent data gap contributes to global inequities in climate impact research and adaptation planning, as small island states and marine-dependent economies are often left out of scenario-based assessments due to a lack of tailored environmental inputs (Barsugli *et al.*, 2013; Drenkard *et al.*, 2021).

This need becomes even more critical when climate data are used to feed ecological and fisheries models. In the context of marine ecosystem modelling, coarse-resolution climate projections from ESMs are often insufficient to capture the fine-scale environmental gradients that structure marine biodiversity, especially in complex coastal and island-rich regions like the South Pacific. This spatial mismatch can compromise the accuracy of ecological models, which require localized inputs to simulate biological responses such as species distribution, habitat suitability, and trophic interactions. High-resolution, bias-corrected data are therefore critical to resolve sub-regional heterogeneity, especially in regions where mesoscale processes (e.g., eddies, upwelling, and shelf dynamics) have disproportionate ecological effects.

For instance, models such as OSMOSE, Atlantis and Ecospace rely on environmental drivers including SST, salinity, and productivity to simulate key life-history processes such as movement, growth, reproduction, and mortality. If these variables are biased or too coarse, the ecological model may either misrepresent species' thermal envelopes or fail to detect critical habitat shifts under climate stress. Thus, robust statistical downscaling and bias correction pipelines are essential to provide input variables that are both realistic in amplitude and locally resolved, enabling reliable assessments of climate impacts and informing the spatial design of marine protected areas or dynamic fisheries management strategies.

High-resolution, bias-corrected SST projections are therefore invaluable: they pinpoint where thermal thresholds are exceeded and where habitat suitability is shifting, informing stakeholders where impacts are likely to intensify and where conservation and adaptation actions should focus. By supplying finely resolved SST projections, this study aims to equip fisheries with the environmental foresight needed for proactive, spatially targeted decision-making under climate change. However, the ability of fisheries science to anticipate these changes depends directly on the accuracy and spatial relevance of the underlying climate data.

Building on recent methodological advancements, we hypothesize that tailoring statistical downscaling and bias correction techniques to the South Pacific's geographic complexity can significantly improve the representation of climate dynamics, particularly in regions characterized by a mix of continental landmasses and small island systems. By aiming to produce high-resolution, bias-corrected climate projections, this study explores whether such refinements can enhance the relevance and usability of climate information for practical applications, such as fisheries management, coastal infrastructure planning, and disaster risk reduction (Teutschbein, Seibert, 2012; Oliveros-Ramos *et al.*, 2025). Despite their importance, statistical downscaling products remain scarce for the South Pacific, and most existing studies have focused on continental regions or have relied on dynamical downscaling techniques (Lal *et al.*, 2008; Chattopadhyay, Katzfey, 2015). The limited availability of regionally tailored downscaling frameworks highlights the need for further

exploration of statistical methods that can capture both the spatial heterogeneity and climate variability unique to small island and coastal systems (Fowler *et al.*, 2007; Xu *et al.*, 2019).
To address the current gap, we build on the methodological framework developed by Oliveros-Ramos et al. (2025), which provides a structured approach for statistical downscaling and bias correction of Earth System Model outputs. We extend this framework by incorporating seasonal predictors and additional environmental covariates such as bathymetry and distance to the continental shelf break. These additions are expected to improve the model's ability to capture fine-scale differences between continental and island climates and possible seasonal trends—an essential distinction for ecological and fisheries applications in the South Pacific, yet often overlooked in large-scale climate models (Drenkard *et al.*, 2021).

The primary objective of this work is to evaluate and compare statistical bias correction and downscaling models for SST in the South Pacific, with a particular focus on the impact of introducing seasonal predictors into the modelling framework. Accurate representation of SST extremes is vital, as these events can cause bleaching, mortality, or reproductive failure in marine organisms (Stoklosa *et al.*, 2015; Oliveros-Ramos *et al.*, 2025). A second objective is to assess progress between successive CMIP rounds (CMIP5 vs CMIP6), highlighting the implications of using the most recent model generation for regional climate applications.

To do so, we implement a multi-step statistical downscaling and bias correction pipeline on a selection of ESMs from both CMIP5 and CMIP6. This design enables us to assess whether CMIP5 models remain competitive for regional applications or if CMIP6 provides substantial improvements. We also compare the legacy RCP scenario framework to the more recent SSP structure (Riahi *et al.*, 2017; Hildén *et al.*, 2018). The choice of climate scenario is itself critical, since it directly frames how future risks are perceived and what types of adaptation strategies are prioritized (Burgess *et al.*, 2023).

This comparative and scenario-diverse approach allows for a more nuanced understanding of future climate risks and their implications across different development trajectories. Global initiatives such as FishMIP have demonstrated how ensembles of ESM-driven scenarios can be operationalized to evaluate marine ecosystem responses and forecast biomass changes (Tittensor *et al.*, 2021). Ultimately, this study tests and refines the statistical downscaling workflow developed by Oliveros-Ramos *et al.*, (2025), applying it in a novel regional context to assess its transferability and enhance its relevance for ecological forecasting and adaptation planning in the tropical Pacific. By delivering operationally relevant, bias-corrected SST products, the project aims to provide the South Pacific fisheries sector with a concrete decision-support tool for managing resources under changing climatic conditions.

2 Materials and Methods

2.1. Observational Data

To serve as the observational baseline for bias correction and statistical modelling, we used the Optimum Interpolation Sea Surface Temperature (OISST**)** dataset, developed by NOAA and distributed by the National Centers for Environmental Information (NCEI). OISST provides global daily fields of sea surface temperature (SST) and sea ice concentration from January 1981 to the present at a spatial resolution of 0.25° × 0.25° (Huang *et al.*, 2021). The product relies on an optimized interpolation method that blends multiple observational sources, including satellite sensors such as the Advanced Very High Resolution Radiometer (AVHRR), drifting buoys, ships, and coastal stations.

This blending ensures continuous, spatially consistent, and accurate SST coverage at both global and regional scales, which is particularly important in data-sparse areas like the South Pacific. Compared to ocean reanalyses such as GLORYS, OISST does not assimilate data into a circulation model, but rather provides a direct observation-based estimate of SST. This characteristic makes it especially robust as a reference for bias correction, since it minimizes dependence on model dynamics while maintaining global consistency and long-term temporal coverage.

Thanks to its fine spatial resolution, global extent, and continuity over more than four decades, OISST represents a well-established and defensible choice for use as the observational baseline in statistical downscaling frameworks aimed at supporting climate and fisheries research.

2.2. Selection of Earth System Models (ESMs)

Earth System Models (ESMs) are comprehensive numerical models that simulate the interactions between the atmosphere, oceans, land surface, cryosphere, and biogeochemical cycles. They are used to project the evolution of the Earth's climate under various forcing conditions, including greenhouse gas emissions and land-use change. ESMs are extensions of General Circulation Models (GCMs), incorporating not only physical processes but also biological and chemical feedback such as the carbon cycle and ocean productivity (Calvin *et al.*, 2023).

To illustrate their internal structure, Figure 1 presents a simplified diagram of ESM components and their interactions. Physical modules (e.g., ocean circulation, atmospheric dynamics) are coupled with biogeochemical components (e.g., nutrient cycling, carbon fluxes), allowing these models to simulate both climatic and ecological variables such as SST, salinity, pH, and chlorophyll.

In this study, we selected ESMs developed by two major climate modelling centres: the *Institut Pierre-Simon Laplace* (IPSL, France) and the *Geophysical Fluid Dynamics Laboratory* (GFDL, United States). Each contributed one model to CMIP5 and one to CMIP6 (Eyring *et al.*, 2016). Specifically, we used IPSL-CM5A-LR (Dufresne et al., 2013) and IPSL-CM6A-LR (Bonnet et al., 2021), together with GFDL-ESM2M (Dunne et al., 2012) and GFDL-ESM4 (Dunne et al., 2020a). These models were selected for their consistent lineage across CMIP generations, their established use in marine applications such as FishMIP and regional impact studies (Eddy et al., 2025), and the availability of both historical and future scenario runs under the RCP and SSP scenarios. Although not exhaustive, this targeted selection allows us to compare the performance and biases of CMIP5 versus CMIP6 frameworks in the South Pacific, particularly for SST, a key driver of ecological and fisheries models. The climate scenarios associated with these models are introduced in **Section 2.3**.

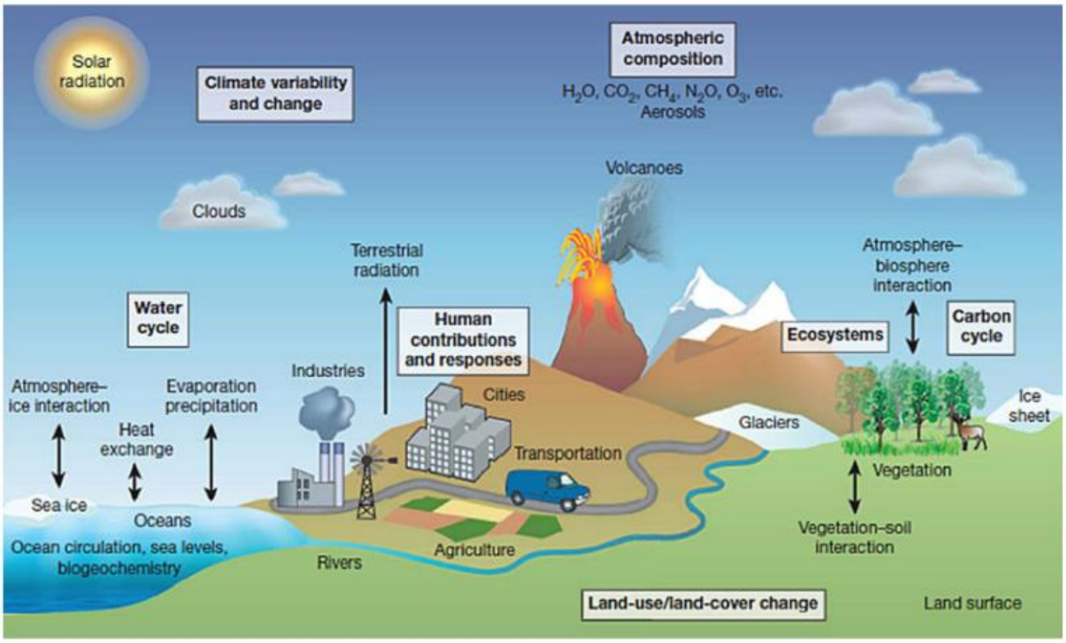

Figure 1. Simplified schematic of Earth System Model components and interactions, including physical climate, carbon, ocean, and atmospheric systems (Dunne *et al.*, 2020a).

2.3. Climate Scenarios : RCPs and SSPs

To explore a range of future climate trajectories, Earth System Models (ESMs) are run under different climate forcing scenarios. These scenarios provide the greenhouse gas concentration pathways that drive simulations of temperature, precipitation, ocean chemistry, and other key variables.

Two main frameworks are used: the Representative Concentration Pathways (RCPs), developed for CMIP5, and the more recent Shared Socioeconomic Pathways (SSPs), used in CMIP6.

RCPs represent different levels of radiative forcing by the year 2100, ranging from strong mitigation (RCP2.6) to high emissions (RCP8.5). They are primarily defined by climate outcomes, without explicit socio-economic context (Van Vuuren *et al.*, 2011).

In contrast, SSPs combine radiative forcing targets with detailed socioeconomic narratives. Each pathway reflects a storyline of global development, integrating factors like inequality, policy implementation, energy use, and land management, which in turn shape both emissions and adaptive capacity (Riahi *et al.*, 2017a; Hildén *et al.*, 2018). The main features of each SSP scenario are summarized in Figure X, which illustrates the different global development trajectories and their implications for mitigation and adaptation. For example, SSP1-2.6 corresponds to a sustainable world with strong mitigation, while SSP5-8.5 assumes development driven by fossil fuels with limited climate action.

In this study, we selected scenario–model combinations that enable a direct comparison between the RCP and SSP frameworks. For CMIP5, we used RCP2.6 and RCP8.5, while for CMIP6 we used SSP1 2.6 and SSP5 8.5.

In addition to the standard RCP–SSP scenario pairs, the IPSL model was also run under the overshoot scenario SSP5-3.4OS. This scenario assumes a temporary exceedance of a 2°C global warming threshold before returning to lower temperature levels by the end of the century through aggressive mitigation efforts. Although SSP5-3.4OS is not yet available for GFDL models, it represents an important addition to fisheries and ecological research, as overshoot trajectories may induce temporary but severe thermal stress events before long-term conditions stabilise. Understanding such transient extremes is essential for designing adaptive strategies that account for both short-term shocks and long-term trends.

This comparative and scenario-diverse approach enables a more nuanced understanding of potential climate futures and their implications for marine ecosystems, fisheries, and adaptation planning in the South Pacific.

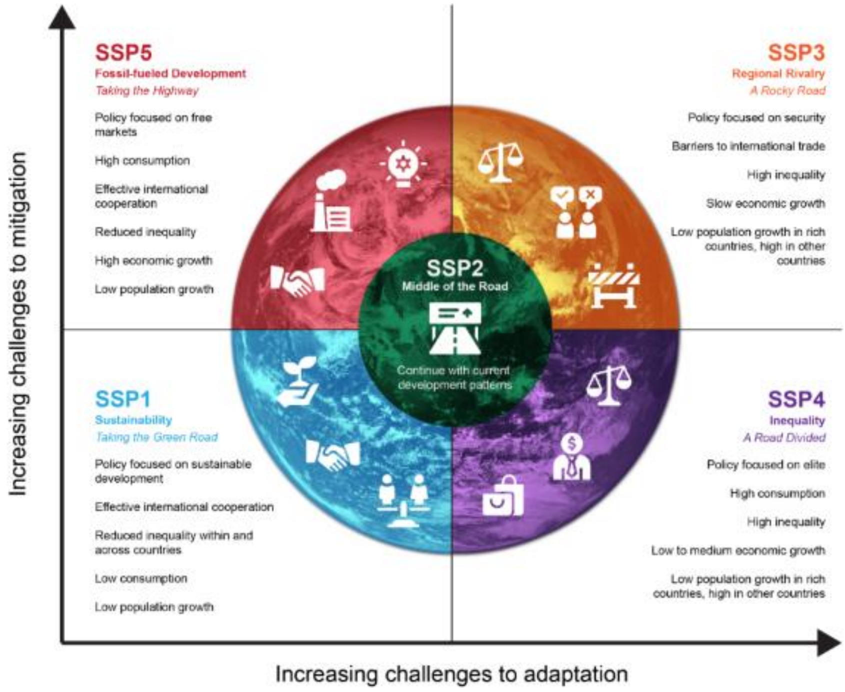

Figure 2. Overview of Shared Socioeconomic Pathways (SSPs), highlighting key narrative features such as policy orientation, inequality, economic growth, and population trends. Adapted from the IPCC SSP framework.

2.4. Methodogy

2.4.1 Downscaling and Bias Correction Workflow

This study applies a multi-step statistical downscaling and bias correction framework adapted from Oliveros-Ramos et al. (2025), with several enhancements tailored to the South Pacific context. The general goal is to produce high-resolution, bias-corrected sea surface temperature (SST) projections from coarse Earth System Model (ESM) outputs, using a combination of empirical distribution mapping and generalized additive models (GAMs). The approach integrates spatial and seasonal covariates to improve performance in areas with strong coastal gradients and seasonal dynamics, features often poorly captured by global models.

The downscaling and correction process follows a structured eight-step protocol (Figure 3) :

Step 1 : Data Subsetting

Model outputs are cropped to the geographic area of interest (South Pacific / SPRFMO area) to reduce computational load and focus on ecologically relevant regions.

Step 2 : Regridding and Harmonization

All model and observational datasets are interpolated to a common spatial resolution of 0.25° × 0.25°, matching the target observational grid (OI-SST).

Step 3 : Quantile Mapping and Bias Characterization

Quantiles of SST distributions are computed for each pixel in both observed and model datasets. This approach captures the structure of bias across the entire distribution, not just the mean, allowing for a more robust correction, especially of extreme values.

Step 4 : Covariate Construction

Spatial and temporal predictors are added to the database. Static variables include bathymetry, expressed as the logarithm of depth, and distance to the shelf break, which is transformed as the sign of the distance multiplied by the logarithm of its absolute value, preserving negative values inside the shelf and positive values outside. Temporal variables include season and month.

Step 5 : Model Training and Cross-Validation

GAMs are trained using subsets of the data following a spatio-temporal cross-validation scheme. Each fold is defined to ensure independence in both space and time, limiting overfitting and allowing a fair evaluation of model skill.

Step 6 : Model Predictions

Once the models were fitted, predictions were generated only on continuous historical and future time series rather than on quantile distributions.

Step 7 : Model Evaluation and Selection

Models are evaluated using a set of indicators grouped into three categories.

Step 8 : Final Model Fitting and Projection

The best-performing model is retrained on the full dataset and used to generate bias-corrected, high-resolution SST projections across the full time period and scenario range (same as step 6).

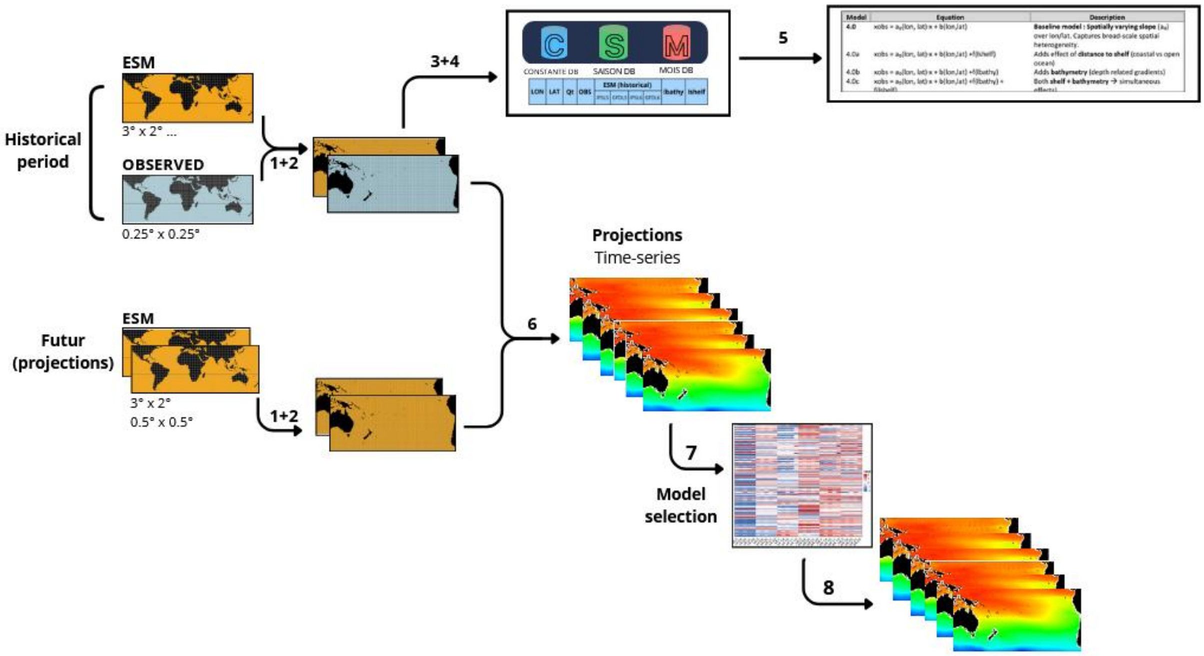

Figure 3. Schematic representation of the statistical downscaling and bias correction workflow, from data extraction and subsetting to database construction, modelling, prediction, evaluation, and final production of bias-corrected SST projections. (adapted from Oliveros-Ramos *et al.*, 2025).

2.4.2 Database Construction and Processing

Spatial Subsetting and Harmonization

To reduce computational costs and focus on ecologically relevant areas, all datasets were spatially restricted to the South Pacific, specifically within the SPRFMO convention area (see Table4). This subsetting allowed the study to target a complex but coherent oceanic zone, while minimizing unnecessary processing outside the region of interest.

Because the observational and model datasets originated from different sources and spatial resolutions, a regridding step was required. All model outputs were interpolated to a common spatial resolution of 0.25° × 0.25° using bilinear interpolation, aligning them with the observational OI-SST grid. This harmonization ensured pixel-level comparability between sources, allowing consistent quantile transformation and modelling procedures across all datasets.
In addition, special care was taken to harmonize longitudinal reference systems. Since some datasets use a –180° to 180° longitude system and others 0° to 360°, all inputs were converted to a common frame to prevent spatial mismatches during interpolation, nearest-neighbour searches, and quantile estimation.

Input Data and Scenario Scope

All Earth System Model (ESM) outputs and observational fields (OISST) were interpolated to a common 0.25° × 0.25° grid to ensure pixel-level comparability. For bias correction, we used historical simulations over 1982–2005 (CMIP5) and 1982–2015 (CMIP6), and future projections under RCP2.6/RCP8.5 (CMIP5) and SSP1-2.6/SSP5-8.5 (CMIP6) (see Table 1 for a summary of input data).

Source	Model & Scenario	Period	Native Resolution	# Data Points	SST (°C)		Dist. to Shelf (km)		Bathymetry (m)	
					Min	Max	Min	Max	Min	Max
OBS	**OISST**	*1982- 2022*	0.25° × 0.25°	29.88 M	-1.80	36.15	-798	5278	-10,315	5685
CMIP5	**IPSL-CM5A-LR** (historical period)	*1982-2005*	3.75° lon × 1.9° lat	55.9 M	-1.93	33.06	-798	5278	-10,315	5685
	IPSL-CM5A-LR (RCP2.6, 8.5)	*2006-2100*	3.75° lon × 1.9° lat	218.3M	-1.93 -1.92	33.72 36.79	-798	5278	-10,315	5685
	GFDL-ESM2M (historical period)	*1982-2005*	2.5° lon × 2.0° lat	55.9M	-1.90	34.81	-798	5278	-10,315	5685
	GFDL-ESM2M (RCP2.6, 8.5)	*2006-2100*	2.5° lon × 2.0° lat	218.3M	-1.89 -1.89	36.32 38.28	-798	5278	-10,315	5685
CMIP6	**IPSL-CM6A-LR** (historical)	*1850-2014*	~100 km ocean grid	76.6M	-2.02	35.12	-798	5278	-10,315	5685
	IPSL-CM6A-LR (SSP1-2.6, 5-8.5)	*2015-2100*	~100 km ocean grid	197.6M	-2.02 -1.20	37.12 39.22	-798	5278	-10,315	5685
	GFDL-ESM4 (historical)	*1850-2014*	0.5° × 0.5°	76.6M	-2.27	36.31	-798	5278	-10,315	5685
	GFDL-ESM4 (SSP1-2.6, 5-8.5)	*2015-2100*	0.5° × 0.5°	197.6M	-2.22 -2.27	37.09 39.05	-798	5278	-10,315	5685

Table 1. Summary of Observational and Model Datasets Used in This Study
Main characteristics of the input data, including period, native resolution, and covariate ranges. All datasets were regridded to a common 0.25° × 0.25° resolution for analysis.

Quantile Computation and Multi-Temporal Databases

Direct chronological comparison between modelled SST from ESMs and observed SST from OI-SST is not possible, because the two time-series are not temporally aligned. While modelled outputs reproduce the seasonal and interannual patterns observed in reality, their time axis represents a alternative climate trajectory within the model rather than true hindcast. This means that comparing SST values at each individual time step would be misleading.

To address this, the comparison between modelled and observed SST was carried out in a distributional framework, using quantiles computed for each grid cell within defined temporal subsets. This approach ensures that bias correction targets the statistical properties of SST mean, variance, and extremes without being affected by temporal phase mismatches.

To explore how temporal structure influences SST modelling, three distinct databases were constructed. The first was a constant database, in which quantiles were computed for each grid cell over the entire historical period without temporal stratification, representing a constant bias structure. The second was a seasonal database, where quantiles were calculated separately for each of the four climatological seasons (JFM, AMJ, JAS, OND), increasing the size of the dataset by a factor of four. The third was a monthly database, in which quantiles were computed by calendar month, increasing the data volume by a factor of twelve while also preserving the cyclic nature of monthly variability.Each database includes 141 quantiles per pixel, spaced more densely near the distribution tails (0.5th to 99.5th percentile in 0.5% steps), capturing detailed SST distribution shapes. The monthly database also includes season labels, allowing flexible modelling with both effects (Figure 4).

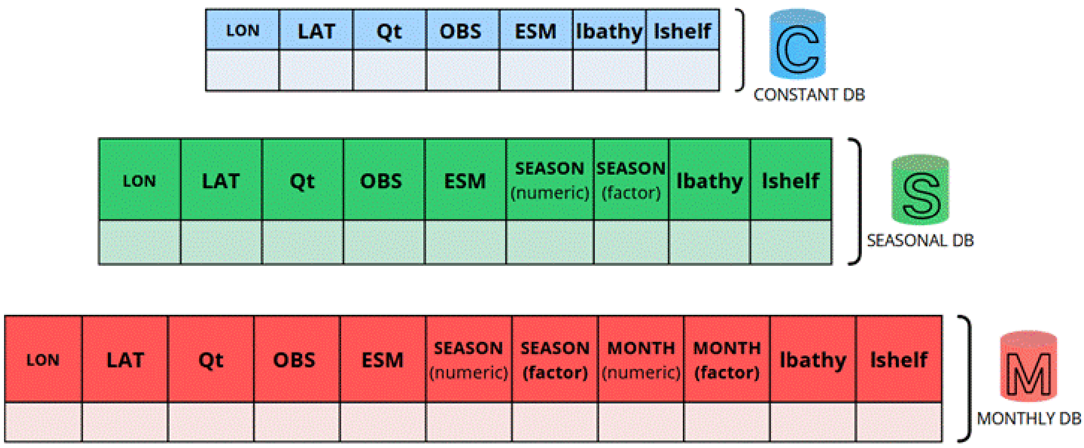

Figure 4. Structure of the constant, seasonal, and monthly databases, showing the addition of time-related covariates and changes in dataset size. Adapted from internal presentation.

Covariates

Covariates were added to all databases to account for spatial and temporal heterogeneity in sea surface temperature. Bathymetry was expressed as the logarithm of depth, while distance to the continental shelf break was calculated as the shortest distance to the 200-metre isobath and transformed as the sign of the distance multiplied by the logarithm of its absolute value, resulting in negative values inside the shelf and positive values offshore.

In addition to these static variables, temporal predictors were introduced in the seasonal and monthly databases. Season and month were represented either as categorical factors, allowing fixed effects, or as cyclic smooths to capture gradual transitions over the annual cycle.

Cross-Validation Design

To assess model robustness and avoid overfitting, each database was split into six non-overlapping folds for spatiotemporal cross-validation. This approach ensured independence in both space and time: five folds were used for training, and one for testing, rotating through all configurations.

Although cross-validation was initially included in the methodological design, it could not be implemented in practice due to lack of storage on the full South Pacific domain. As a result, final model fitting was performed on the complete datasets after CV testing, and a summary of the estimated storage costs with and without CV is provided in Annex III.

Use of Multi-Database Framework

This framework allowed us to test different hypotheses regarding the role of temporal detail in downscaling performance. Because the covariate structure was held constant across all datasets, we could directly assess the added value of seasonal and monthly granularity under identical spatial conditions. This flexibility is crucial for understanding how temporal dynamics influence the reliability of bias correction and SST projections.

2.4.3. Statistical Model Design and Implementation

For this study, we focused on a structured family of statistical models derived from Model 4, which balances interpretability and flexibility. Conceptually, Model 4 represents the statistical relationship between simulated and observed SST quantiles: it is essentially a regression where the slope of the predictor (simulated SST) is allowed to vary spatially and temporally. This formulation makes it the simplest possible bias-correction model while already accounting for key sources of heterogeneity.

The baseline formulation (Model 4.0) includes spatially varying slopes across longitude and latitude, with a smooth offset term. From this foundation, additional predictors were progressively included: bathymetry, distance to the shelf break, and their interaction. Temporal stratification was introduced in two alternative forms, with slopes varying by season (Models 4.1a–d) or by month (Models 4.2a–d). This incremental structure allowed us to evaluate the contribution of each covariate and temporal resolution to model skill while maintaining a parsimonious and consistent framework.

Applied systematically across the three database structures (constant, seasonal, monthly), this resulted in a total of 30 fitted models (5 for the constant database, 10 for the seasonal database, and 15 for the monthly database). By restricting the analysis to this model family, we emphasize the use of a transparent, regression-based approach while still exploring meaningful ecological and physical drivers of SST bias.

More complex nonlinear structures were not retained here but are presented in the Perspectives as avenues for future work. For clarity, a detailed summary of all model formulations (4.0–4.2 with covariate variants a–d) is provided in Table 2, with explicit equations and covariate descriptions.

Model	Equation	Description
4.0	xobs = a_0(lon, lat)·x + b(lon,lat)	**Baseline model : Spatially varying slope** (a_0) over lon/lat. Captures broad-scale spatial heterogeneity.
4.0a	xobs = a_0(lon, lat)·x + b(lon,lat) +f(lshelf)	Adds effect of **distance to shelf** (coastal vs open ocean)
4.0b	xobs = a_0(lon, lat)·x + b(lon,lat) +f(lbathy)	Adds **bathymetry** (depth related gradients)
4.0c	xobs = a_0(lon, lat)·x + b(lon,lat) +f(lbathy) + f(lshelf)	Both **shelf + bathymetry** → simultaneous effects)
4.0d	xobs = a_0(lon, lat)·x + b(lon,lat) + f(lbathy) + f(lshelf) + f(lbathy,lshelf)	Same as 4.0c + **interaction** between **shelf** and **bathymetry**
4.1	xobs = a_0(lon, lat, season)·x + b(lon,lat)	**Seasonal variation** in spatial slope (one slope per season). Extension of **4.0**
4.1a	xobs = a_0(lon, lat, season)·x + b(lon,lat) +f(lshelf)	Seasonal model with additional **shelf-distance** effects.
4.1b	xobs = a_0(lon, lat, season)·x + b(lon,lat) +f(lbathy)	Same as 4.1a but with **bathymetry.**
4.1c	xobs = a_0(lon, lat, season)·x + b(lon,lat) +f(lbathy) + f(lshelf)	Seasonal model combining both **bathymetry** and **shelf distance**.
4.1d	xobs = a_0(lon, lat, season)·x + b(lon,lat) + f(lbathy) + f(lshelf) + f(lbathy,lshelf)	Seasonal model with **both covariates** and their **interaction**.
4.2	xobs = a_0(lon, lat, month)·x + b(lon,lat)	**Monthly variation** in spatial slope (one slope per month). Extension of **4.0**
4.2a	xobs = a_0(lon, lat, month)·x + b(lon,lat) +f(lshelf)	Monthly model with additional shelf-distance effects
4.2b	xobs = a_0(lon, lat, month)·x + b(lon,lat) +f(lbathy)	Same as 4.2a but with **bathymetry.**
4.2c	xobs = a_0(lon, lat, month)·x + b(lon,lat) +f(lbathy) + f(lshelf)	Monthly model combining both **bathymetry** and **shelf distance**.
4.2d	xobs = a_0(lon, lat, month)·x + b(lon,lat) + f(lbathy) + f(lshelf) + f(lbathy,lshelf)	**Most complex model**: monthly stratification plus **bathymetry**, **shelf distance**, and their **interaction**.

Table 2. Mathematical formulation and interpretation of the 30 variants of Model 4 used in this study. These models include progressively more complex spatial covariates (bathymetry, shelf distance, and their interaction) and temporal structures (constant, seasonal, monthly).

Model Naming Convention and Structure

To facilitate systematic comparison, each model was labelled using a standard code that combined the database type (c, s, or m), the model structure number (4.0, 4.1, or 4.2), and, when relevant, a covariate suffix (a–d). The database prefix indicated whether quantiles were computed at the constant, seasonal, or monthly scale. The model number referred to the temporal structure of the slope, with 4.0 denoting constant slopes, 4.1 seasonal slopes, and 4.2 monthly slopes. Finally, the covariate suffix specified the progressive addition of bathymetry, distance to the continental shelf, or their interaction. The naming scheme is summarized in Figure 5.

To optimize computational efficiency, we implemented parallel processing for model fitting. Each database was processed separately using a dedicated script, and each modelling task was submitted using 24 cores per run. Within each run, we set *nthreads = 4* in the *bam()* function after initial testing showed this provided the best trade-off between memory usage and speed. This parallelization allowed each model to be fitted across multiple subsets concurrently and significantly reduced computation time compared to using *gam()* without parallelization, especially for the monthly database.

While the exact internal distribution of parallel tasks across folds is handled automatically by bam(), our tests confirmed that this configuration consistently produced stable and fast results.

Prefix = DATABASE	**c**	**s**	**m**
Model Number	4	4	4
Seasonality ? (0:2)	c4.0 ~~c4.1~~ ~~c4.2~~	s4.0 s4.1 ~~s4.2~~	m4.0 m4.1 m4.2
Covariates ? (a:d)	c4.0a c4.0b c4.0c c4.0d	s4.0a s4.0b s4.0c s4.0d	m4.0a m4.0b m4.0c m4.0d

Figure 5. Model naming convention used throughout the study. Prefixes refer to the database type (c = constant, s = seasonal, m = monthly), followed by the model number and optional covariate configuration suffix (a–d).

2.4.4 Model predictions

The prediction stage was adapted to ensure comparability across all database structures (constant, seasonal, monthly). Instead of predicting quantile distributions directly, an approach initially considered but computationally prohibitive at the scale of the South Pacific, models were only applied to the complete historical and future time series for each grid cell. From these predicted time series, the relevant statistical properties (mean, 5th, and 95th percentiles) were recomputed a posteriori.

These recomputed quantiles provided the necessary inputs for the evaluation indicators, including residuals, explained deviance, and future bias. This adjustment preserved the statistical basis of the evaluation framework, ensured that results were comparable across databases, and significantly reduced both computational costs and storage demands.

2.4.5. Model Evaluation and Selection

Model evaluation was conducted using a structured set of indicators, adapted from Oliveros-Ramos et al. (2025), and grouped into three categories (Table 3): (A) future bias indicators, (B) residual and present bias indicators, and (C) explained deviance indicators. These were computed not only across the full South Pacific but also within ecologically or climatically relevant subregions (e.g., Niño3.4, Niño1+2, shelf vs offshore zones, warm vs cold sectors). This regional breakdown allowed us to detect spatial variation in model skill, particularly in sensitive areas such as ENSO hotspots or narrow shelf systems.

To facilitate understanding of the evaluation framework, schematic maps of some subregions are provided in Annex V. These maps illustrate the spatial boundaries of each subset (e.g., Niño regions, continental shelf, upwelling zones), complementing the indicator definitions presented in Table 3.

Category	Indicators	Purpose
Future Bias	A1–A70 (cold/hot range, mean, spread, change)	Test model realism in future SSTs
Residuals & Bias	B1–B16 (MAE, asymmetry, tails, Niño bias)	Evaluate fit under observed SSTs
Explained Deviance	C1 + regional subsets (e.g., shelf, ENSO zones)	Assess variance explained

Table 3. Summary of model evaluation indicators by category. For full definitions, spatial coverage, and equations, see Annex V.

A. Future Bias Indicators

Future bias indicators assess errors under future conditions by comparing corrected projections with raw ESM outputs. Since no observations exist for the future, these metrics focus on internal consistency rather than direct fit. They evaluate model reliability under different climate scenarios (RCP2.6/SSP1-2.6 and RCP8.5/SSP5-8.5), focusing on changes in the range and mean of cold and warm SST extremes across the global domain, as well as regional biases in Niño3.4 and Niño1+2. They also include scenario deltas, which highlight differences between mitigation and high-emission futures. Together, these indicators help detect structural overfitting to historical SST and provide insight into the stability of models when exposed to strong warming or mitigation scenarios.

B. Present Bias and Residual Indicators

Present bias and residual indicators evaluate direct comparisons between corrected models and observations in the historical period. They capture both global properties such as mean absolute error, residual range, asymmetry, and conditional tail expectations, as well as regional residuals in Niño3.4 and Niño1+2 that emphasize biases and asymmetry in ENSO-sensitive zones. These are true residuals, since they are based on observed versus simulated SST. Together, they ensure that central tendencies and distribution tails are represented, while also revealing whether models drift consistently in sensitive regions.

C. Explained Deviance Indicators

Explained deviance indicators quantify the proportion of variance explained relative to a null model (mod0.0), providing an overall measure of model skill. They were computed not only for the full dataset but also for subregions, including cold and warm temperature zones, shallow versus deep waters, shelf versus open ocean, and key sectors such as the Niño regions, Australia, and the South American coast. This approach made it possible to identify models that perform well overall but fail in specific ecological hotspots, which is particularly important for fisheries applications. For consistency, deviance was transformed so that a value of 0 represents the best performance and 1 the worst (i.e., 1 – deviance explained).

Together, these three categories provide a comprehensive evaluation framework: A tests stability and plausibility in the future, B measures fit against observations in the present, and C captures variance explained across scales.

Indicator Normalization and Ranking Procedure

To ensure comparability across indicators of different scale and units, all metrics were first aligned so that lower values consistently represent better performance. This harmonization avoids contradictory directions between categories (e.g., some indicators increasing with performance and others decreasing).

Once aligned and after subsetting them for each ESM, the indicators were normalized using the scale function, which centers and scales values across models so that they fall within a comparable range (approximately –2 to 2). This transformation standardizes the relative variation of each indicator without altering their relative ranking within a given model subset.

Rather than computing a composite score or ranking, the normalized indicators were retained for multi-criteria evaluation. They were used to generate heatmaps and spatial diagnostics, allowing us to identify strengths and weaknesses of each model across categories (bias, residuals, explained deviance).
The full list of indicators, their formulas, units, and spatial definitions is available in Annex V.

2.5. Final Downscaling and Projections

Following the model evaluation and ranking process (Section 2.4.4), the best-performing model from each database (constant, seasonal, and monthly) was retrained on the full dataset to maximize information use and statistical power. These final models were then used to produce bias-corrected SST projections over the full future period (2006–2100).

The bias correction was applied to monthly SST outputs from each selected Earth System Model (ESM), under the following climate scenarios:

- CMIP5: RCP2.6 and RCP8.5
- CMIP6: SSP1-2.6, SSP5-8.5, and SSP5-3.4OS (for IPSL)

The models were applied to each scenario separately using the same spatial and covariate structure used in training, ensuring consistency between observed and projected domains. Future ESM SST values were input into the trained models, which returned corrected SST estimates at 0.25° resolution for each pixel and month.

All predictions were stored in NetCDF format with standardized metadata, compatible with downstream ecological modelling tools such as Ecospace, or OSMOSE, and formatted to facilitate mapping, indicator computation, or integration into fisheries risk assessments.
The projections produced include:

- Bias-corrected SST time series (2006–2100) for each ESM × scenario combination,
- Outputs from three modelling strategies (constant, seasonal, monthly) for comparison,

- Full spatial coverage of the SPRFMO region and surrounding South Pacific zones.

These outputs allow future analyses to explore spatial SST trends, detect extreme events, and compute indicators of climate vulnerability or ecological risk.

Although this phase focused primarily on SST projections, the downscaling framework developed is flexible and can be applied to other variables (e.g., salinity, oxygen, pH) if reanalysis data are available.

2.6. Methodological Challenge : Model Comparison and Visualisation

Comparing the performance of 30 statistical models against more than 100 indicators quickly posed a significant visualization and interpretation challenge. With such a large number of metrics, traditional approaches such as spider plots became impractical and unreadable. This difficulty was amplified by the fact that models differed in their covariate structure and temporal formulation (constant, seasonal, monthly), making direct comparisons even harder.

To address this issue, we reorganized the evaluation framework around heatmaps, which allow performance to be compactly summarized across indicators, scenarios, and subregions. This visualization strategy highlights trade-offs between metrics (e.g., bias, residual spread, explained deviance) and makes it easier to detect anomalous cases that warrant further investigation.

The scale of the South Pacific application also required workflow and memory optimisations, including parallelisation and modular scripting, which are discussed in Section 4 (“Synthesis of Challenges”, “Synthesis of Contributions”).

3 Results

3.1 Reduction/ Distribution of the Bias

To illustrate the effect of statistical correction, we first examine spatial bias maps for each ESM generation. These maps compare raw simulations against two representative downscaling models, across the 5th, 50th, and 95th quantiles. They provide a spatially explicit perspective on whether downscaling reduces systematic errors and how these improvements vary across model generations and quantiles.

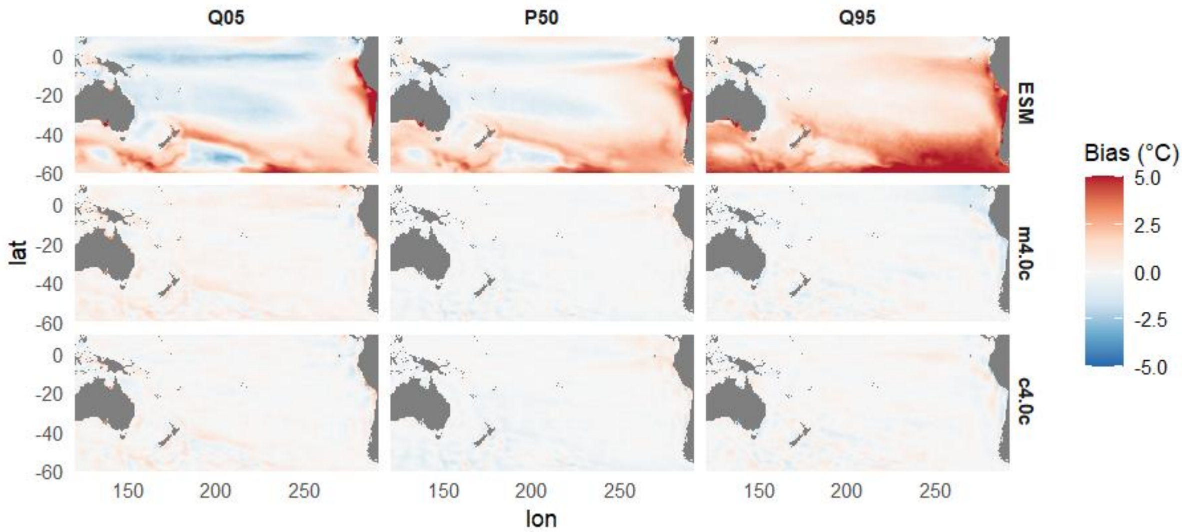

Figure 6. Bias map of GFDL CMIP5 (compares the raw ESM biases with those corrected by two representative models ;m4.0c and c4.0c; for the 5th, 50th, and 95th quantiles over the historical period 1981-2005)

GFDL CMIP5 (Figure 6) shows a strong warm bias in the raw simulation, particularly at high quantiles (Q95), where anomalies exceed +5 °C in parts of the equatorial Pacific. These errors are most pronounced in ENSO-sensitive regions and eastern boundary upwelling zones, consistent with known CMIP5 limitations. Both corrected models (m4.0c and c4.0c) substantially reduce these biases across quantiles, bringing values close to zero except for localized residuals. Importantly, improvements extend beyond the mean state (P50) to extremes (Q05, Q95), confirming the value of a quantile-based approach.

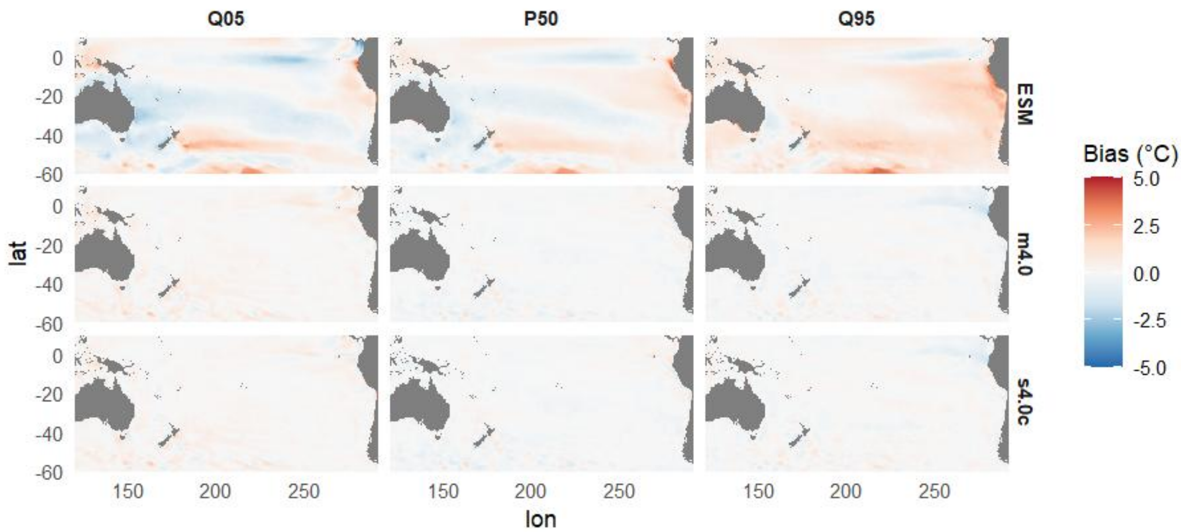

Figure 7. Bias map of GFDL CMIP6 (compares the raw ESM biases with those corrected by two representative models ;m4.0 and s4.0c; for the 5th, 50th, and 95th quantiles over the historical period 1981-2005)

GFDL CMIP6 (Figure 7) already performs better than its CMIP5 predecessor, with reduced basin-wide warm anomalies, especially at Q95. This reflects advances in model physics and resolution (Dunne *et* *al.*, 2020b). Nonetheless, residual errors persist in equatorial and coastal regions. Downscaling (m4.0 and s4.0c) further improves these fields, effectively correcting both mean and extreme values. Differences between monthly and seasonal formulations are subtle, aligning with heatmap results that showed only marginal added value of temporal stratification for this model.

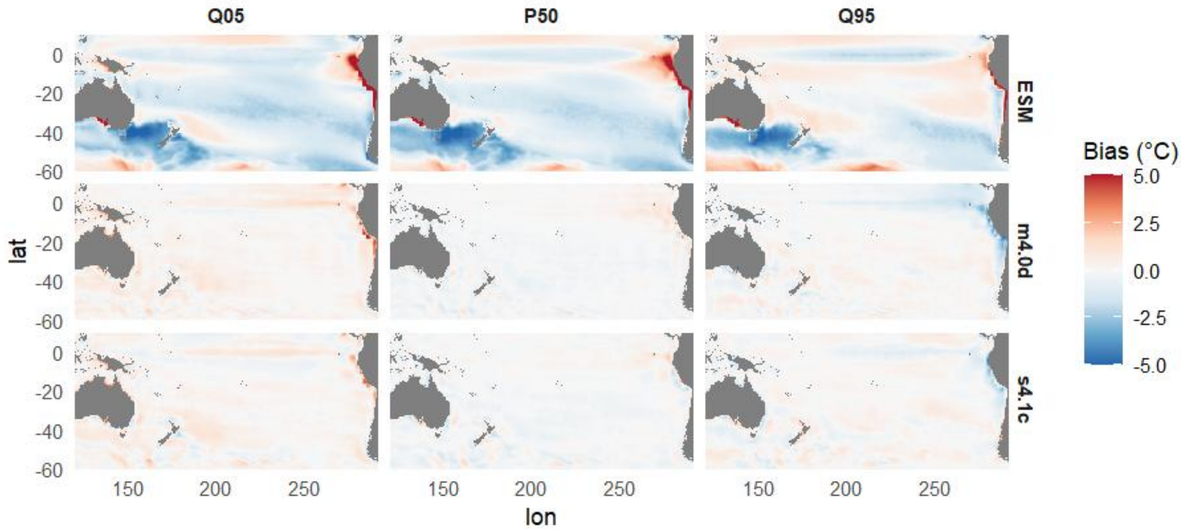

Figure 8. Bias map of IPSL CMIP5 (compares the raw ESM biases with those corrected by two representative models ;m4.0d and s4.1c; for the 5th, 50th, and 95th quantiles over the historical period 1981-2005)

IPSL CMIP5 (Figure 8) displays widespread cold biases, especially at Q05 and P50, with localized warm anomalies near the eastern boundary. Correction with m4.0d and s4.1c reduces these systematic errors, but residual anomalies remain in equatorial and coastal regions. Seasonal predictors appear to offer slight benefits, echoing indicator results that suggested modest gains for IPSL CMIP5 when seasonality is included.

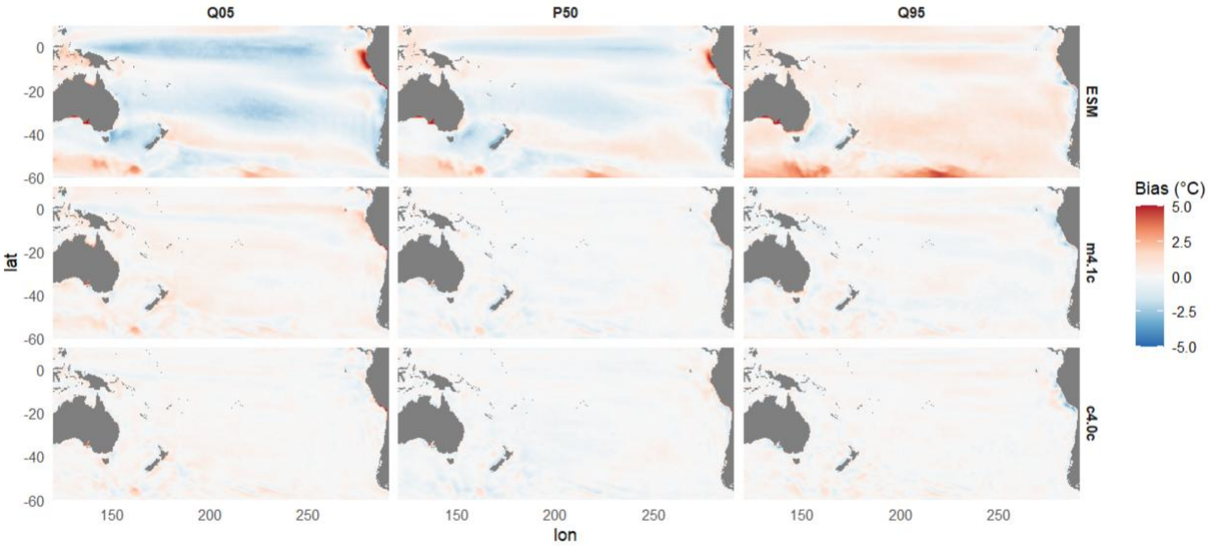

Figure 9. Bias map of IPSL CMIP6 (compares the raw ESM biases with those corrected by two representative models ;m4.1c and c4.0c; for the 5th, 50th, and 95th quantiles over the historical period 1981-2005)

IPSL CMIP6 (Figure 9) shows clear improvements relative to CMIP5, with weaker cold anomalies and closer agreement with observations. However, equatorial and nearshore biases remain. Among the corrected models, c4.0c provides consistently stable results across quantiles, while m4.0 introduces localized inconsistencies despite correcting some large-scale errors. This highlights that even within improved CMIP6 models, the stability of statistical correction can vary depending on the formulation.

Taken together, these maps demonstrate three key points: (i) bias correction strongly improves both mean and extreme SST estimates relative to raw ESMs; (ii) CMIP6 generally outperforms CMIP5 at the raw stage, reducing the scale of errors before correction; and (iii) downscaling formulations differ in their stability, with some leaving localized inconsistencies in sensitive regions such as the equator and coastal upwellings. These observations motivate a more systematic comparison using indicator-based evaluations, to assess whether visual improvements in maps align with quantitative measures of performance across regions and scenarios.

Despite the overall improvements, the corrected models still exhibit localized issues. Residual warm and cold anomalies remain particularly in equatorial ENSO regions (Niño3.4, Niño1+2) and along the Peruvian coast, where strong upwelling makes SST patterns difficult to reproduce. These areas are ecologically and climatically critical, meaning that even small biases may have disproportionate consequences for fisheries and ecosystem projections.

Because such differences are not always evident from visual inspection alone, we next turn to a systematic indicator-based evaluation. The heatmaps presented in Section 3.2 quantify model skill across bias categories (future errors, present residuals, explained deviance) and across regions, allowing us to test whether the visual improvements seen in the maps are consistent, robust, and ecologically meaningful.

3.2 Indicator-Based Evaluation

The bias maps highlighted strong large-scale improvements after correction, but also persistent bias in ENSO regions and upwelling zones. To analyse these differences more systematically, we used indicator heatmaps (Figure 10). For readability, we grouped the indicators into three categories: A (future bias errors, by subset: all, q05, q95, Niño3.4, Niño1+2), B (residuals, present vs observations), and C (unexplained deviance).

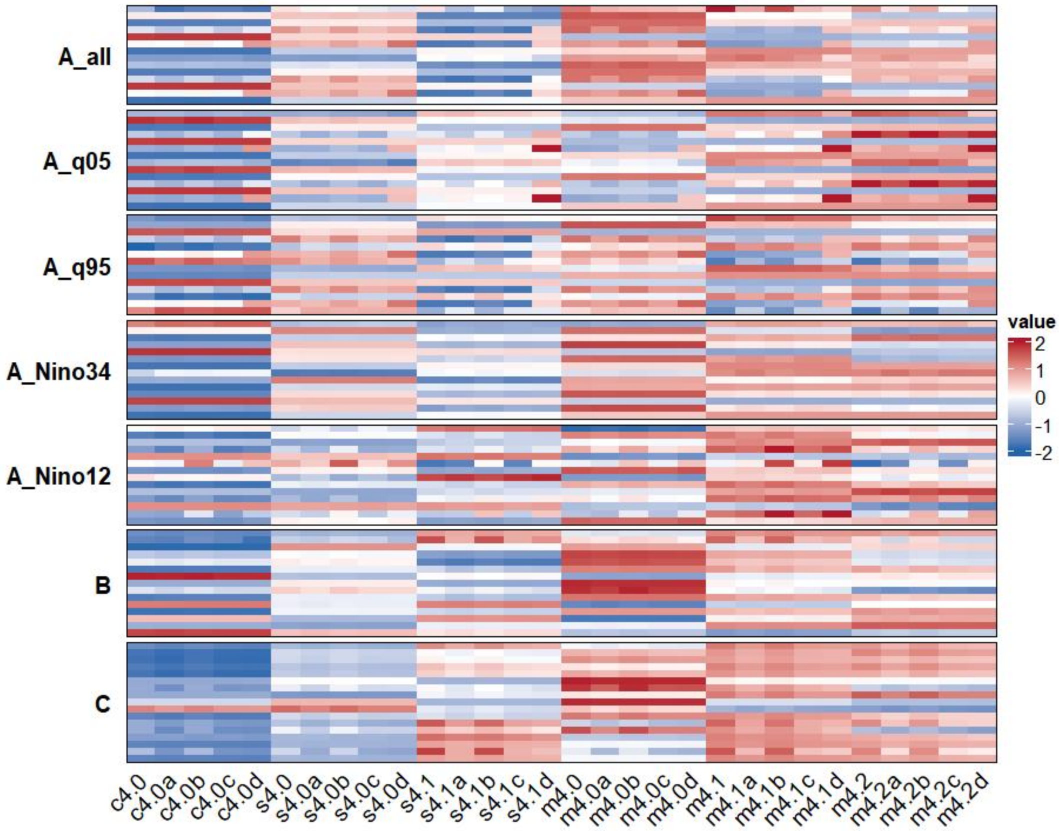

Figure 10. Heatmap of indicators for GFDL CMIP5 Earth System Model

Because the full heatmaps are dense, we interpret them here through three complementary “levels of reading”: (i) the role of covariates, (ii) the effect of database structure, and (iii) the added value of seasonality in the correction formula. The complete set of heatmaps is provided in Annex VI.

The role of covariates

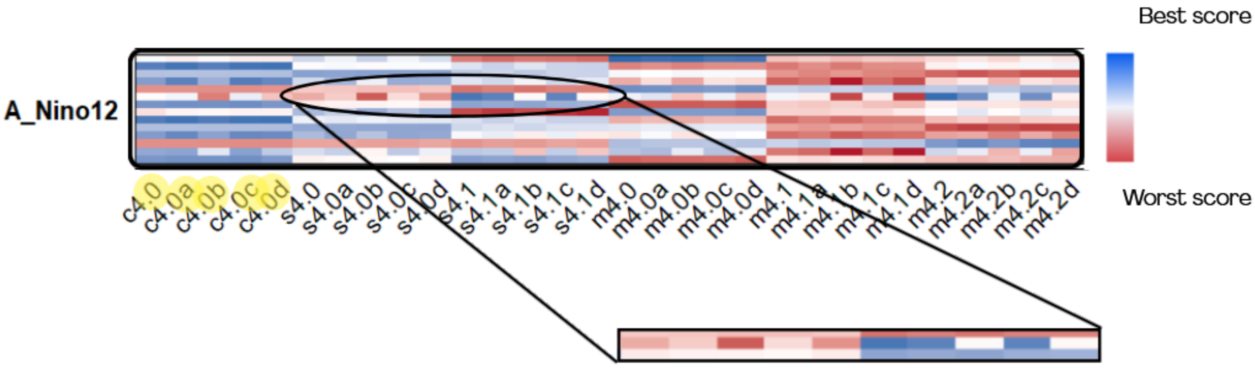

Figure 11. Zoom on Heatmap of indicators for GFDL CMIP5 Earth System Model

Looking first at the role of geographic covariates, the full heatmap (Figure 10) shows that performance varies strongly depending on whether bathymetry or shelf-related predictors are included. To clarify this effect, we zoomed on the indicator A Niño1+2 subset (Figure 11), which is particularly sensitive to equatorial and coastal biases. The zoom reveals that the best-performing formulations are those including distance to the continental shelf (covariate set a), with further improvements when combined with bathymetry (set c). By contrast, models using only bathymetry (b) or the full interaction between shelf and bathymetry (d) consistently perform worse.

This first level of analysis indicates that distance to the shelf break is a key predictor for improving statistical correction, particularly when combined with bathymetry, while more complex interaction terms tend to introduce instability.

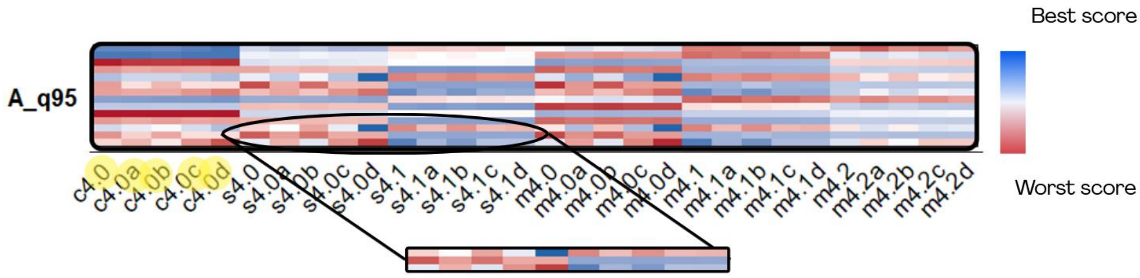

Figure 12. Zoom on Heatmap of indicators for GFDL CMIP6 Earth System Model

An additional nuance emerges when comparing different A-type indicators (Figure 12). While covariates such as shelf distance and bathymetry often improve average bias metrics (e.g. A4, A5), their effect is less consistent for worst-case indicators (A6, A7). In several cases, the inclusion of covariates reduces the mean magnitude of outliers but simultaneously introduces localized instabilities, which worsen the maximum residuals detected by A6–A7. This discrepancy highlights the trade-off between optimizing overall model stability and minimizing extreme deviations.

From a practical perspective, this means that the choice of covariates, and more broadly, of “best” models, depends on the intended application. If the objective is to reduce mean bias across the basin, geographic covariates provide clear benefits. However, if the priority is to avoid large localized errors that could drive ecological thresholds, simpler models may sometimes be preferable. This reinforces the idea that indicator selection should be aligned with research objectives: whether the focus is on average conditions or on extremes that can trigger ecological impacts.

The effect of database structure

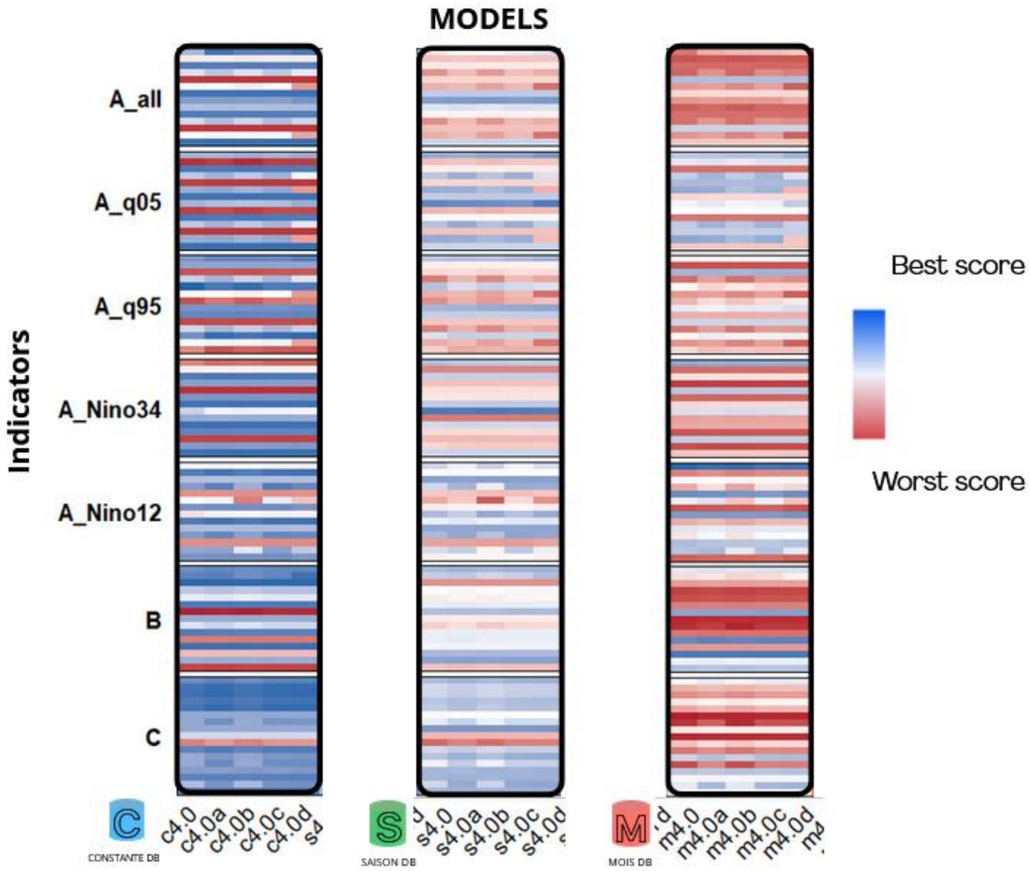

Figure 13. Zoom on Heatmap of indicators for GFDL CMIP5 Earth System Model

The second level of interpretation concerns the impact of database stratification (constant vs seasonal vs monthly). The full heatmaps show that simply splitting the database into seasonal (s4.0) or monthly (m4.0) subsets rarely improves performance relative to the constant database (c4.0). In some cases, stratification even degrades results (Figure 13), particularly in ENSO-sensitive regions. This pattern suggests that, in models such as GFDL CMIP5 and IPSL CMIP5, the raw seasonal cycle is not sufficiently well captured by the ESMs to benefit from stratification alone.

However, a closer look reveals that for nearly every red line (poor score) in the constant-database models, performance improves when the database is stratified, and the best scores are often found in the monthly database formulations. This is especially visible for type A indicators, where structuring the data by month (or season) captures certain aspects of variability more effectively. In particular, constant models perform poorly for minimum SST indicators (A3, A5, A7), which are biologically critical extremes, while stratified models better represent these conditions. Similarly, residuals remain high in ENSO subsets (B indicators) and unexplained variance is elevated outside those zones (C indicators), confirming that constant-database models are insufficient to capture the complexity of South Pacific variability.

In other words, database stratification alone is not a guarantee of improvement, but it can add meaningful information for extremes and ENSO-sensitive dynamics, with monthly stratification often providing the clearest gains.

The added value of seasonality in the correction formula

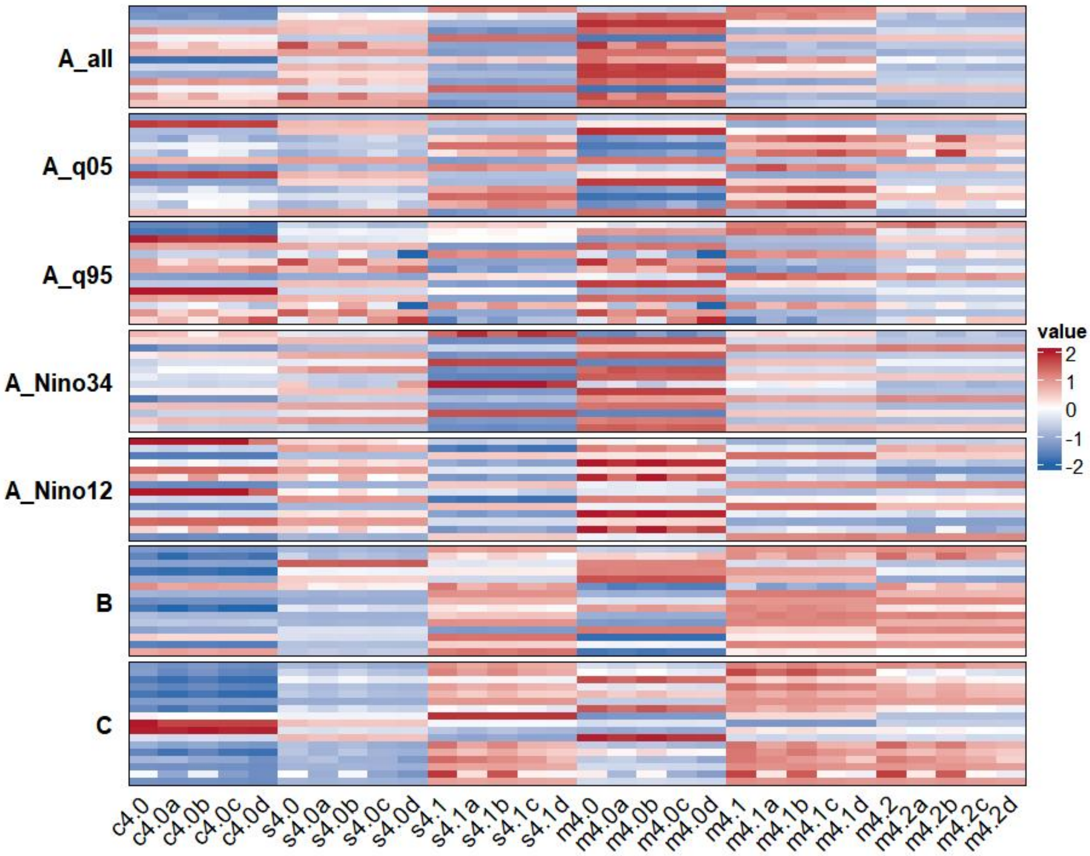

Figure 14. Heatmap of indicators for GFDL CMIP6 Earth System Model

The third level of interpretation examines whether including seasonality directly in the correction function improves performance. To explore this, we focused on CMIP6 results (Figure 14), where the raw ESMs already capture the seasonal cycle more realistically than CMIP5. Zooms on ENSO regions (Niño3.4, Niño1+2) and on distribution tails (Q05, Q95) confirm that models explicitly including seasonality as a covariate (s4.1, m4.1, m4.2) often outperform their counterparts based only on database stratification (s4.0, m4.0). These formulations tend to reduce errors in extreme quantiles and improve stability in ENSO-sensitive regions, both of which are critical for ecological applications.

However, the gains remain heterogeneous, and their impact depends on the indicator family considered. In several cases, seasonal models improve the representation of extremes and ENSO subsets (higher A scores) but do so at the expense of overall deviance explained (lower C scores). Conversely, models that maximize deviance explained may leave substantial residual errors in extremes or sensitive regions. This creates a clear trade-off between correcting future bias errors (A) and optimizing global model fit (C).

Overall, this third level of reading suggests that including seasonality in the formula can bring added value, especially for newer ESM generations such as CMIP6, where seasonal dynamics are better resolved. Yet, the effect is context-dependent and does not remove the need for spatial diagnostics. In practical terms, a model with excellent deviance scores but poor ENSO correction may not be ecologically reliable, while a model that reduces extremes but explains less variance globally may still be valuable for fisheries-focused applications where thermal thresholds drive impacts.

Therefore, no single formulation emerges as universally optimal across all indicators. The choice of a "best" model depends on the intended application: models emphasizing extremes and ENSO may be preferable for ecological risk assessments, whereas those maximizing explained deviance may be more suitable for general climate projections. This trade-off justifies complementing indicator heatmaps with spatial bias maps, which provide a direct view of where residual errors remain and whether they overlap with ecologically critical areas.

3.3 Best model?

At this stage, it is difficult to single out a "best" model across the ensemble. With 30 candidate structures and over a hundred indicators, visualization remains a key challenge: while heatmaps highlight relative strengths and weaknesses, they do not provide a straightforward way to rank or classify models in a consistent manner. This limitation will be discussed further in Section 4, where we consider possible strategies for model grouping or selection.

Rather than attempting to force a final choice here, we turn to complementary diagnostics : time-series comparisons, to specifically assess how downscaling affects long-term SST trajectories under different climate scenarios. These plots provide a more intuitive view of whether correction schemes align historical simulations with observations and how they propagate into future projections.

3.4 Time series

While indicator heatmaps and bias maps provide insight into spatial patterns and model performance across categories, they do not show how corrections affect the temporal evolution of SST. To address this, we next compare time series of non bias-corrected and bias-corrected SST for all selected ESMs under two climate scenarios: RCP2.6/SSP1-2.6 (strong mitigation) and RCP8.5/SSP5-8.5 (high emissions). For consistency, the same statistical model was applied across all ESMs, allowing differences between scenarios and model generations (CMIP5 vs. CMIP6) to emerge more clearly.

These plots serve two purposes: first, to check whether bias correction successfully aligns the historical period with observations, and second, to highlight how future SST trajectories diverge under mitigation versus high-emission pathways. This temporal perspective complements the indicator- and map-based diagnostics by showing how differences in bias correction propagate through time.

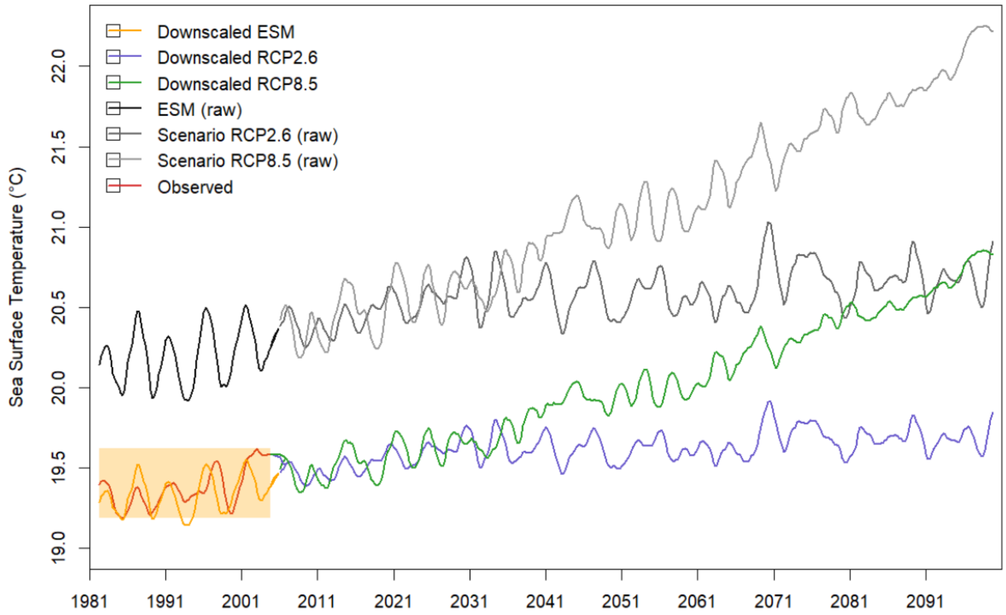

Figure 15. Time series of SST (IPSL CMIP5) for the South Pacific from 1982 to 2100, comparing observed OISST, raw ESM simulations (historical and future under RCP2.6 and RCP8.5), and downscaled projections.

The time series (Figure 15) illustrates the impact of statistical downscaling and bias correction for IPSL CMIP5 across the historical and projected periods. The raw IPSL simulation (black) shows a pronounced warm bias relative to observations (red), with historical SSTs consistently overestimated. The corrected historical series (orange) substantially reduces this offset, aligning the climatological baseline much more closely with observations.

It is important to note that corrected simulations cannot reproduce the exact year-to-year observed variability, since ESM historical runs represent internally generated “fictive” timelines. Comparisons are therefore valid in terms of statistical properties (mean, variance, extremes) rather than exact chronology.

The corrected projections (blue: RCP2.6, green: RCP8.5) retain alignment with the observed baseline while diverging strongly depending on the emissions pathway. Although the corrections appear modest in absolute terms, even shifts on the order of 1 °C are ecologically significant: many marine species show nonlinear responses near thermal thresholds, with consequences for recruitment, distribution, and life-history processes (Johansen *et al.*, 2024; Lindmark *et al.*, 2022).

Interestingly, the bias structure is not the same across modelling centres: while IPSL CMIP5 is too warm, GFDL CMIP5 (shown in Annex VII) is systematically too cold in the historical period. These opposite raw biases highlight the importance of comparing multiple ESMs and correcting them before use in ecological applications.

This figure underlines the dual role of downscaling: correcting systematic model biases in the historical baseline, and ensuring that projected warming trajectories are framed against ecologically meaningful reference conditions.

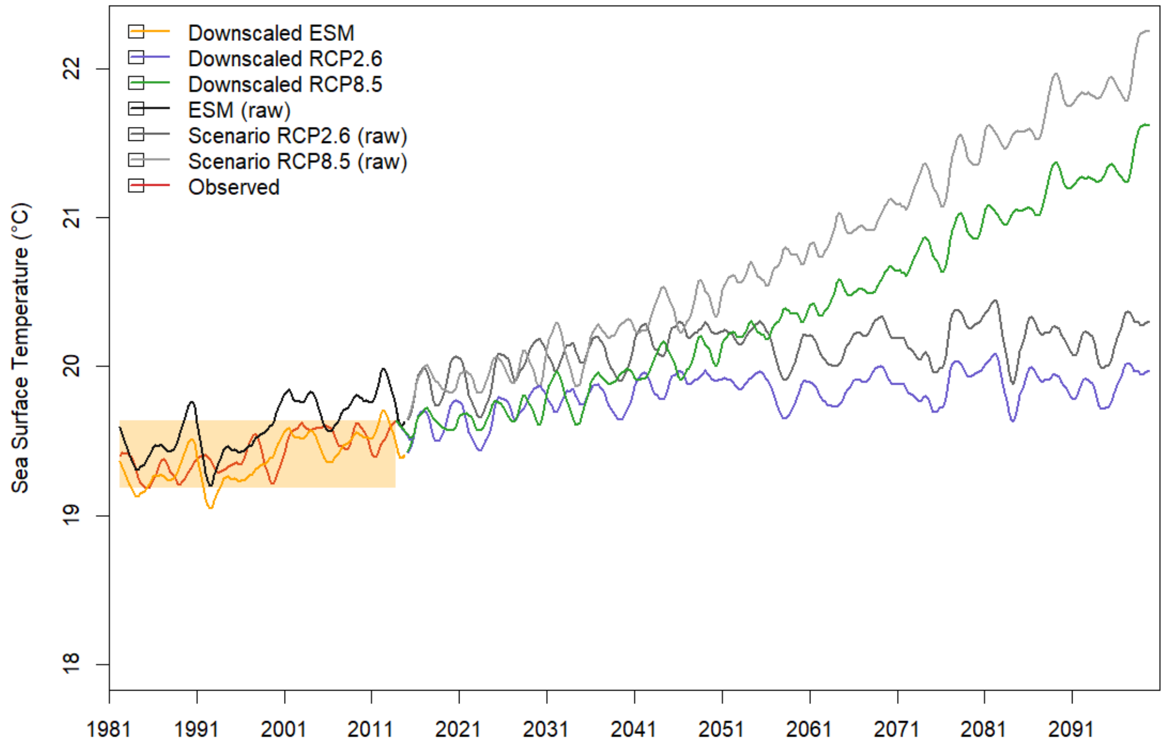

Figure 16. Time-series for GFDL CMIP6 ESM (historical + future scenario) raw and downscaled projections.

In contrast to the strong warm bias seen in IPSL CMIP5, the CMIP6 version shows markedly reduced historical errors (Figure 16), with raw simulations already closer to observations. Bias correction therefore requires smaller adjustments, and the corrected trajectories remain more stable through time. Under RCP2.6/SSP1-2.6, SST increases moderately before stabilizing after mid-century, whereas under RCP8.5/SSP5-8.5, a steep upward trend persists. The clearer alignment of IPSL CMIP6 with observations highlights the generational improvement between CMIP5 and CMIP6 and demonstrates how newer models provide a more robust foundation for statistical downscaling.

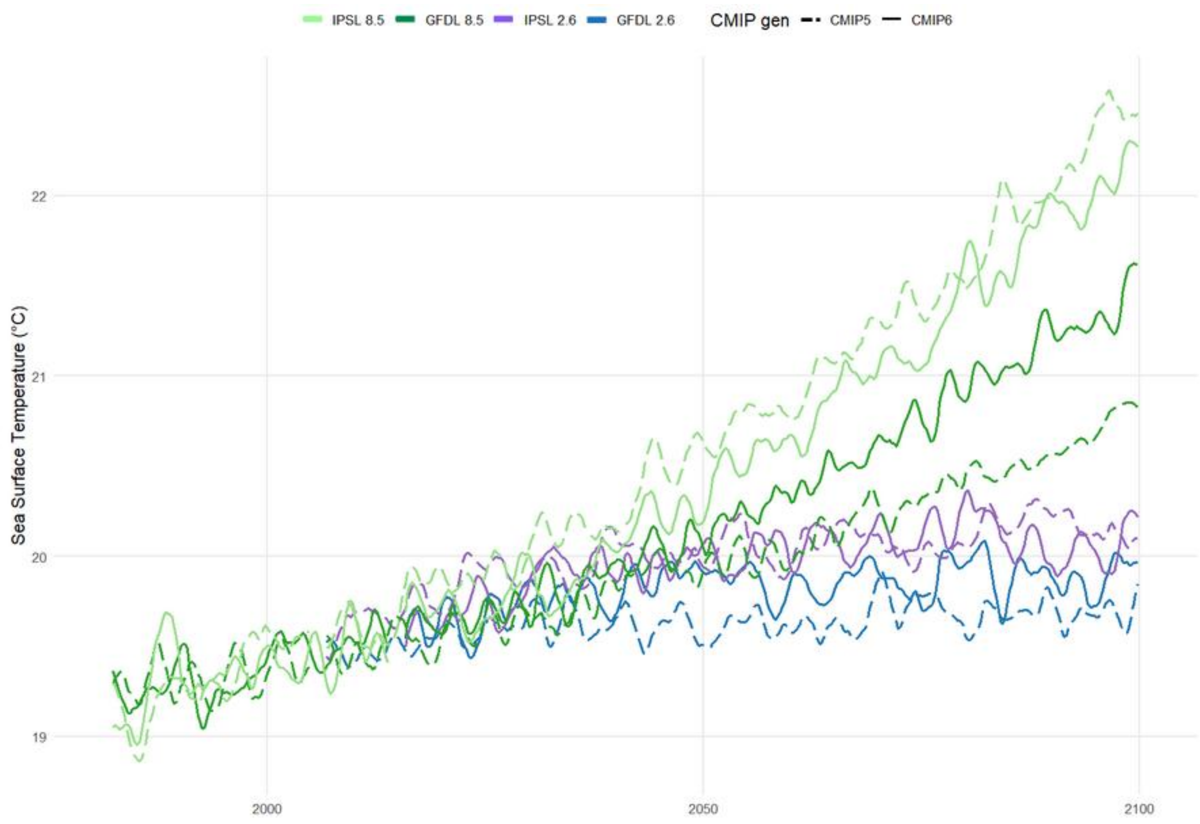

Figure 17. Time series of sea surface temperature (SST) for the South Pacific from 1982 to 2100, comparing observed OISST and all ESM downscaled projections (historical and future under RCP/SSP2.6 and RCP/SSP8.5) for model c4.0c.

Figure 17 presents the aggregated downscaled time series for all ESMs. Under RCP2.6/SSP1-2.6, SST increases moderately before stabilizing after mid-century, with models converging toward a narrow band. This stabilization illustrates the potential of strong mitigation to limit warming, although ecosystems remain exposed to sustained pressure compared to the historical baseline. In contrast, under RCP8.5/SSP5-8.5, SST rises steeply throughout the century, diverging by several degrees relative to the low-emission case by 2100. Model spread also increases, reflecting larger uncertainty under high warming. This trajectory pushes South Pacific SST far outside its historical envelope, amplifying risks such as coral bleaching, fish distribution shifts, and declines in fisheries yields.

Although the numerical corrections appear modest (often <1 °C), these differences are ecologically significant. Marine fish and invertebrates exhibit strong thermal sensitivity, with nonlinear responses of metabolism, growth, and recruitment near threshold temperatures (Johansen et al., 2024; Lindmark et al., 2022). The corrected projections therefore provide a more realistic baseline against which to assess ecological vulnerability.

The comparison between IPSL and GFDL further highlights the importance of model generation. In CMIP5, IPSL simulations are systematically too warm in the historical period, while GFDL simulations are too cold. These opposite biases propagate into the future, complicating direct scenario comparisons and making raw outputs unsuitable for ecological analyses.

By contrast, CMIP6 shows clear improvements. Historical SSTs are much closer to the observed climatology, reducing the correction needed and producing more stable projections. This is particularly evident for IPSL CMIP6 (Figure 17), where downscaled historical SST aligns closely with observations, and future trajectories remain consistent with scenario expectations. For GFDL CMIP6 (see Annex VII), improvements are also visible, although some discrepancies remain in the representation of the seasonal cycle.

These results confirm that bias correction is more effective when applied to newer ESM generations, as the raw inputs already provide a realistic climatological baseline. At the same time, differences between modelling centres persist even within CMIP6, underlining the importance of using multiple ESMs rather than relying on a single source for regional climate assessments.

4 Discussion

Synthesis of Challenges

The scale of this project, covering the entire South Pacific, multiple climate scenarios, and large SST databases, required several workflow adaptations to make the analysis feasible on HPC infrastructure. Many computational challenges only became apparent after moving from the small, localised domain used during the initial methodology familiarisation phase to the full South Pacific domain. The larger domain greatly increased data volume, spatial heterogeneity, and processing time, exposing bottlenecks in RAM usage, I/O speed, and model storage that were not encountered at smaller scales. The most significant of these were:

- Memory-efficient processing : Removing intermediate objects *(rm(), gc()),* subsetting datasets in chunks, and avoiding unnecessary storage of large temporary files.
- Parallelized GAM/BAM fitting : Using *bam()* with *nthreads = 4* and distributing subsets across 24 cores to dramatically reduce runtime (Oedekoven *et al.*, 2023), with *gam()* used only when necessary for null models.
- Model object compression : Implementing a *compact gam()* function to strip unnecessary elements from fitted models, reducing .rds size by up to two orders of magnitude.
- Switch from CSV to *Parquet* (*arrow* package): Using a compact, compressed columnar format for climate datasets, reducing file size, speeding up read/write operations, and allowing selective loading of variables (Abdelaziz *et al.*, 2024).
- Modular and reproducible code structure : Standardizing naming conventions, separating scripts by workflow stage (import, processing, fitting, evaluation), and ensuring traceability across all models and scenarios.
- Storage space limitations : Unlike RAM or runtime, which could be managed with workflow optimisations, storage space remained a hard limitation (Schnase *et al.*, 2016). The size of the South Pacific domain and the need to run multiple model variants generated terabytes of outputs, preventing us from systematically storing cross-validation runs and quantile predictions.

While most of the above challenges were addressed through workflow optimisation, the storage issue required a methodological adjustment (Schnase *et al.*, 2016). Specifically, predictions were carried out on full time series rather than on quantiles, with quantiles recomputed a posteriori for indicator evaluation. This change ensured comparability across databases while reducing storage demands to a manageable level.

Full descriptions, implementation details, and performance gains for each of these strategies are provided in Appendix VII.

Synthesis of Contributions

This study advances statistical downscaling and bias correction for marine climate applications in the South Pacific through the following contributions:

- Adaptation of an existing downscaling framework ; The methodology of Oliveros-Ramos et al. (2025) was adapted to the South Pacific, a geographically complex and data-sparse region dominated by small islands, steep bathymetry, and diverse oceanographic conditions.
- Integration of seasonal predictors : Seasonal and monthly predictors were incorporated into the modelling framework to explicitly evaluate the added value of temporal structure in bias correction, enabling systematic comparison of models with varying temporal granularity.
- Model comparison across CMIP generations : Paired models from CMIP5 and CMIP6 (IPSL and GFDL) were used to directly assess progress between model generations, providing evidence on whether newer ESMs offer measurable improvements for regional-scale applications.
- Application to fisheries-relevant climate indicators : A tailored suite of indicators was developed to evaluate model performance with a focus on metrics directly relevant to fisheries management, such as shifts in extreme SST events and biases in key ecological regions (e.g., Niño boxes, coastal areas).

By combining these methodological advances, the study delivers high-resolution, bias-corrected SST projections tailored to the South Pacific. These outputs provide fisheries managers and other stakeholders with actionable information on where and when critical thermal thresholds may be exceeded, helping to anticipate shifts in fish distribution, identify areas at risk of stock decline, and design spatially targeted adaptation and conservation strategies (Hobday *et al.*, 2018). This aligns with recent efforts to integrate climate scenarios into fisheries and aquaculture management (Hollowed *et al.*, 2025), underlining the value of downscaled SST products as operational inputs for developing climate-informed strategies in marine resource governance.

Challenges in model identification

A central difficulty highlighted by this study is the challenge of identifying a single “best” model. With 103 indicators evaluated across 30 model structures, no candidate consistently outperformed the others across all categories and regions. Some models showed strong results for broad-scale indicators but weaknesses in ENSO-sensitive zones, while others performed well in Niño regions but introduced residual biases elsewhere. This heterogeneity reflects both the complexity of the South Pacific domain and the limitations of individual indicators, which often emphasize different aspects of model skill.

Rather than selecting one optimal model, our results underscore the need for multi-criteria evaluation frameworks and complementary diagnostics (heatmaps, bias maps, time series) that can highlight trade-offs. This approach provides a more transparent view of strengths and weaknesses, and it avoids the pitfalls of over-reliance on a single ranking metric. Future work could explore formal strategies for model classification or weighting, but for now the main outcome is a framework that helps reduce the model space while retaining flexibility for ecological applications.

An additional implication is that the choice of indicators must be explicitly aligned with the goals of a study. Our results show that models performing well on average bias indicators (e.g. A4–A5) do not always achieve the best scores on extreme or worst-case metrics (A6–A7), and vice versa. This means that selecting a "best" model depends not only on technical performance but also on the intended application: global climate analyses may prioritize explained variance and mean errors, while fisheries or ecological risk assessments may require a stronger emphasis on extremes and ENSO-sensitive regions. Recognizing this trade-off is essential for tailoring downscaling outputs to the specific needs of end-users.

Perspectives

Other model implemetation

Beyond the restricted set of Model 4 variants implemented in this study, the broader downscaling framework originally developed by Oliveros-Ramos et al. (2025) allows for a much wider exploration of model structures. To illustrate the potential of this framework, Table 4 presents the full catalogue of candidate models, ranging from simple linear corrections to more complex formulations including nonlinear corrections, interaction terms, and higher-order spatial effects. These models were not applied here due to computational and storage constraints, but they remain part of the methodological roadmap. With the covariates and seasonality variations it would have taken us rom 30 to 216 models. Their inclusion highlights clear avenues for future research, where expanded model spaces could be systematically tested to evaluate trade-offs between parsimony, flexibility, and predictive accuracy.

Bias structure study

A perspective for future work would be to study the structure of the bias itself before engaging in large-scale model fitting. Exploring how biases vary spatially, temporally, and across covariates could help identify systematic patterns in the raw ESM–observation differences. Such an analysis might allow the pre-selection of the most relevant model structures, thereby reducing both computational cost and storage requirements by avoiding redundant model testing. Implementing this strategy would require a dedicated methodological effort focused on bias characterization, which was beyond the scope of this study, but could ultimately lead to more efficient and targeted downscaling pipelines.

Modelling domain variation

Another perspective concerns the definition of the modelling domain. In this work, the South Pacific was treated as a single coherent region, which allowed for basin-wide coverage but inevitably reduced the capacity to capture fine-scale patterns. The results confirmed that model skill is not uniform across the domain: some models performed well at large scale but struggled in ENSO-sensitive regions (e.g., Niño regions), while others corrected biases locally but introduced inconsistencies elsewhere. This heterogeneity, combined with the large number of indicators (103) and model structures (30), made it difficult to identify a single "best" model and highlighted the importance of multi-criteria evaluation.

An alternative strategy would be to subdivide the domain into smaller, ecologically or climatically relevant subregions. For example, ENSO regions, the Peruvian upwelling system, or island-rich areas; and either combine these together afterwards or focus corrections specifically where performance is weakest. Such a subregional approach could balance local accuracy in complex nearshore environments with the large-scale coherence required for basin-wide projections. A first illustration of this strategy is provided in Annex VIII, which shows a proposed subdivision of the Pacific into distinct zones, developed in parallel by another intern project.

Model visualization and selection

Another important challenge concerns the visualization and selection of models. With 30 model structures and 103 indicators, identifying a single best candidate remains difficult. Heatmaps provided a useful way to summarize this large amount of information, making trade-offs and anomalies more visible. Although widely used in other fields (such as genetics and molecular biology, where they support the classification of DNA sequences) heatmaps have rarely been applied to statistical downscaling in climate sciences. Future work should therefore explore complementary approaches, such as ranking procedures, clustering, or dendrograms, to better structure model inter-comparisons and move toward systematic selection strategies.

Overshoot scenarios as a priority for future work

Finally, while overshoot scenarios such as SSP5-3.4OS were secondary and optional in CMIP6 derived simulation workflows, they have been made principal scenarios in CMIP7, reflecting the growing recognition of their importance in understanding long-term climate trajectories. Overshoot pathways are particularly relevant because they capture futures where global temperatures temporarily exceed a critical threshold (e.g., 1.5 °C or 2 °C) before returning to lower levels, allowing assessment of both the impacts during the overshoot and the potential for recovery. These scenarios may be among the most informative for fisheries and ecosystem-based management, as they combine the short-term risks of extreme warming with the long-term potential for adaptation or regeneration. Extending statistical downscaling efforts to a broader range of overshoot scenarios, and over their longer temporal horizons, would provide a more complete picture of future risks and resilience for South Pacific marine systems.

Model	Equation	Description
0.0	$xobs = x + b_0$	**Global mean bias correction** (null model); b_0 is a constant offset.
0.1	$xobs = x + f(season) + b_0$	**Same as 0.0, but bias varies by season;** b_0 is a constant.
0.2	$xobs = x + f(month) + b_0$	**Same as 0.0, but bias varies by month**; b_0 is a constant.
1.0	$xobs = x + b(...)$	**Smooth spatial mean bias correction;** b is a smooth function of lon/lat.
1.1	$xobs = x + f(season) + b(...)$	**Same as 1.0, with an added fixed seasonal effect** (season as factor).
1.2	$xobs = x + f(month) + b(...)$	**Same as 1.0, with an added fixed monthly effect** (month as factor).
2.0	$xobs = a_{11} \cdot x + b(...)$	**Global linear correction**; a_{11} is a constant slope.
2.1	$xobs = a_{11}(season) \cdot x + f(season) + b(...)$	**Season-specific slope** and **intercept**; captures seasonal amplitude and mean variation.
2.2	$xobs = a_{11}(month) \cdot x + f(month) + b(...)$	**Month-specific slope** and **intercept**; captures monthly amplitude and variation.
3.0	$xobs = a_{11}(x) + b(...)$	**Global non-linear correction**; a_{11} is a smooth function of x.
3.1	$xobs = a_{11}(x) + a_{11}(season)(x) + f(season) + b(...)$	Adds **season-specific** smooth **corrections**.
3.2	$xobs = a_{11}(x) + a_{11}(month)(x) + f(month) + b(...)$	Adds **month-specific** smooth **corrections**.
4.0	$xobs = a_0(lon, lat) \cdot x + b(...)$	**Spatially varying slope** (a_0) over lon/lat; b is a smooth offset.
4.1	$xobs = a_0(lon, lat, season) \cdot x + b(...)$	**Seasonal variation** in spatial slope (one slope per season).
4.2	$xobs = a_0(lon, lat, month) \cdot x + b(...)$	**Monthly variation** in spatial slope (one slope per month).
5.0	$xobs = a_0(lon, lat) \cdot x + a_{11}(x) + b(...)$	**Spatially varying slope** (4.0) plus **global non-linear correction**.
5.1	$xobs = a_0(lon, lat, season) \cdot x + a_{11}(x) + b(...)$	Adds **seasonal variation** to spatial slope (as in 4.1) plus non-linear term.
5.2	$xobs = a_0(lon, lat, month) \cdot x + a_{11}(x) + b(...)$	Adds **monthly variation** to spatial slope (as in 4.2) plus non-linear term.
6.0	$xobs = a_{01}(lon) \cdot x + a_{02}(lat) \cdot x + b(...)$	**Additive spatially varying slope** components (lon and lat treated separately).
6.1	$xobs = a_{01}(lon, season) \cdot x + a_{02}(lat, season) \cdot x + b(...)$	Adds **seasonal variation** to each slope component.
6.2	$xobs = a_{01}(lon, month) \cdot x + a_{02}(lat, month) \cdot x + b(...)$	Adds **monthly variation** to each slope component.
7.0	$xobs = (a_{11} + a_{12} \cdot lon + a_{13} \cdot lat) \cdot x + b(...)$	**Additive linear slope** correction using lon and lat as fixed effects.
7.1	$xobs = (a_{11} + a_{12} \cdot lon + a_{13} \cdot lat + a_{14} \cdot season + a_{15} \cdot lon \cdot season + a_{16} \cdot lat \cdot season) \cdot x + b(...)$	Adds **seasonal interactions** with lon and lat; captures seasonal spatial **gradients**.
7.2	$xobs = (a_{11} + a_{12} \cdot lon + a_{13} \cdot lat + a_{14} \cdot month + a_{15} \cdot lon \cdot month + a_{16} \cdot lat \cdot month) \cdot x + b(...)$	Adds **monthly interactions** with lon and lat; captures monthly spatial **gradients**.

Table 4. Mathematical formulation and interpretation of the 25 statistical model structures used in this study. Models include varying levels of complexity in bias correction: global vs. spatial, linear vs. non-linear, and temporal structures (seasonal/monthly) either as fixed effects or smooth interactions.

5 Conclusion

This study developed and tested a statistical downscaling and bias correction framework for sea surface temperature (SST) in the South Pacific, comparing CMIP5 and CMIP6 models across multiple database structures and covariates (Annex VI). With 30 models and 103 indicators, the analysis demonstrated that no single configuration consistently outperformed the others: strengths in one set of indicators or regions often came at the cost of weaknesses elsewhere. In other words, one size does not fit all. This reflects both the diversity of climatic regimes in the South Pacific and the fact that indicator choice shapes which models appear most skilful.

A key implication is that model evaluation must be goal-dependent. Indicators optimized for mean bias may not align with those targeting extremes, and the “best” model will differ depending on whether the focus is global climate diagnostics or fisheries-oriented risk assessments. This reinforces the need for flexible, multi-criteria frameworks rather than a single ranking, and for tailoring evaluation to the specific priorities of end-users.

A promising direction is therefore to build smaller, subregion-focused models. For example, targeting ENSO hotspots, the Peruvian upwelling system, or island-rich areas and later merging them into a basin-wide ensemble. Such an approach would capture the ecological and climatic specificities of each area while still providing coherent projections at the scale needed for management bodies like the SPRFMO.

In this context, future climate scenarios, particularly overshoot pathways now prioritized in CMIP7, add urgency. These scenarios, where global temperatures temporarily exceed thresholds such as +1.5 °C or +2 °C before declining again, are likely to produce short but intense shocks. For fisheries, the spatial unevenness of these shocks means that regionalized models are especially valuable: they allow us to identify where impacts will be most acute, where recovery may be possible, and how management strategies should be adapted at both local and basin scale.

By combining regional tailoring with expanded scenario coverage, statistical downscaling can provide fisheries and conservation actors with the fine-scale, ecologically relevant climate information needed to anticipate risks, plan adaptation, and safeguard the resilience of South Pacific marine systems.

Bibliography

ABDELAZIZ, Abdullah I., HANSON, Kent A., GABER, Charles E. et LEE, Todd A., 2024. Optimizing large real-world data analysis with parquet files in R: A step-by-step tutorial. *Pharmacoepidemiology and Drug Safety*. 2024. Vol. 33, n° 3, pp. e5728. DOI 10.1002/pds.5728.

AHMED, Kazi Farzan, WANG, Guiling, SILANDER, John, WILSON, Adam M., ALLEN, Jenica M., HORTON, Radley et ANYAH, Richard, 2013. Statistical downscaling and bias correction of climate model outputs for climate change impact assessment in the U.S. northeast. *Global and Planetary Change*. 1 janvier 2013. Vol. 100, pp. 320-332. DOI 10.1016/j.gloplacha.2012.11.003.

BARSUGLI, Joseph J., GUENTCHEV, Galina, HORTON, Radley M., WOOD, Andrew, MEARNS, Linda O., LIANG, Xin-Zhong, WINKLER, Julie A., DIXON, Keith, HAYHOE, Katharine, ROOD, Richard B., GODDARD, Lisa, RAY, Andrea, BUJA, Lawrence et AMMANN, Caspar, 2013. The Practitioner's Dilemma: How to Assess the Credibility of Downscaled Climate Projections. *Eos, Transactions American Geophysical Union*. 2013. Vol. 94, n° 46, pp. 424-425. DOI 10.1002/2013EO460005.

BURGESS, M G, BECKER, S L, LANGENDORF, R E, FREDSTON, A et BROOKS, C M, 2023. Climate change scenarios in fisheries and aquatic conservation research. *ICES Journal of Marine Science*. 1 juillet 2023. Vol. 80, n° 5, pp. 1163-1178. DOI 10.1093/icesjms/fsad045.

CALVIN, Katherine, DASGUPTA, Dipak, KRINNER, Gerhard, MUKHERJI, Aditi, THORNE, Peter W., TRISOS, Christopher, ROMERO, José, ALDUNCE, Paulina, BARRETT, Ko, BLANCO, Gabriel, CHEUNG, William W.L., CONNORS, Sarah, DENTON, Fatima, DIONGUE-NIANG, Aïda, DODMAN, David, GARSCHAGEN, Matthias, GEDEN, Oliver, HAYWARD, Bronwyn, JONES, Christopher, JOTZO, Frank, KRUG, Thelma, LASCO, Rodel, LEE, Yune-Yi, MASSON-DELMOTTE, Valérie, MEINSHAUSEN, Malte, MINTENBECK, Katja, MOKSSIT, Abdalah, OTTO, Friederike E.L., PATHAK, Minal, PIRANI, Anna, POLOCZANSKA, Elvira, PÖRTNER, Hans-Otto, REVI, Aromar, ROBERTS, Debra C., ROY, Joyashree, RUANE, Alex C., SKEA, Jim, SHUKLA, Priyadarshi R., SLADE, Raphael, SLANGEN, Aimée, SOKONA, Youba, SÖRENSSON, Anna A., TIGNOR, Melinda, VAN VUUREN, Detlef, WEI, Yi-Ming, WINKLER, Harald, ZHAI, Panmao, ZOMMERS, Zinta, HOURCADE, Jean-Charles, JOHNSON, Francis X., PACHAURI, Shonali, SIMPSON, Nicholas P., SINGH, Chandni, THOMAS, Adelle, TOTIN, Edmond, ARIAS, Paola, BUSTAMANTE, Mercedes, ELGIZOULI, Ismail, FLATO, Gregory, HOWDEN, Mark, MÉNDEZ-VALLEJO, Carlos, PEREIRA, Joy Jacqueline, PICHS-MADRUGA, Ramón, ROSE, Steven K., SAHEB, Yamina, SÁNCHEZ RODRÍGUEZ, Roberto, ÜRGE-VORSATZ, Diana, XIAO, Cunde, YASSAA, Noureddine, ALEGRÍA, Andrés, ARMOUR, Kyle, BEDNAR-FRIEDL, Birgit, BLOK, Kornelis, CISSÉ, Guéladio, DENTENER, Frank, ERIKSEN, Siri, FISCHER, Erich, GARNER, Gregory, GUIVARCH, Céline, HAASNOOT, Marjolijn, HANSEN, Gerrit, HAUSER, Mathias, HAWKINS, Ed, HERMANS, Tim, KOPP, Robert, LEPRINCE-RINGUET, Noëmie, LEWIS, Jared, LEY, Debora, LUDDEN, Chloé, NIAMIR, Leila, NICHOLLS, Zebedee, SOME, Shreya, SZOPA, Sophie, TREWIN, Blair, VAN DER WIJST, Kaj-Ivar, WINTER, Gundula, WITTING, Maximilian, BIRT, Arlene, HA, Meeyoung, ROMERO, José, KIM, Jinmi, HAITES, Erik F., JUNG, Yonghun, STAVINS, Robert, BIRT, Arlene, HA, Meeyoung, ORENDAIN, Dan Jezreel A., IGNON, Lance, PARK, Semin, PARK, Youngin, REISINGER, Andy, CAMMARAMO, Diego, FISCHLIN, Andreas, FUGLESTVEDT, Jan S., HANSEN, Gerrit, LUDDEN, Chloé, MASSON-DELMOTTE, Valérie, MATTHEWS, J.B. Robin, MINTENBECK, Katja, PIRANI, Anna, POLOCZANSKA, Elvira, LEPRINCE-RINGUET, Noëmie et PÉAN, Clotilde, 2023. *IPCC, 2023: Climate Change 2023: Synthesis Report. Contribution of Working Groups I, II and III to the Sixth Assessment Report of the Intergovernmental Panel on Climate Change [Core Writing Team, H. Lee and J. Romero (eds.)]. IPCC, Geneva, Switzerland.* [en ligne]. First. Intergovernmental Panel on Climate Change (IPCC). [Consulté le 6 août 2025]. Disponible à l'adresse : https://www.ipcc.ch/report/ar6/syr/

CANNON, Alex J., PIANI, Claudio et SIPPEL, Sebastian, 2020. Bias correction of climate model output for impact models. In : *Climate Extremes and Their Implications for Impact and Risk Assessment* [en ligne]. Elsevier. pp. 77-104. [Consulté le 27 mars 2025]. ISBN 978-0-12-814895-2. Disponible à l'adresse : https://linkinghub.elsevier.com/retrieve/pii/B9780128148952000057

CHATTOPADHYAY, Mohar et KATZFEY, Jack, 2015. Simulating the climate of South Pacific islands using a high resolution model. *International Journal of Climatology*. 2015. Vol. 35, n° 6, pp. 1157-1171. DOI 10.1002/joc.4046.

CHRISTENSEN, Villy, PIRODDI, Chiara, COLL, Marta, STEENBEEK, Jeroen, BUSZOWSKI, Joe et DANIEL, Pauly, 2011. Fish biomass in the world ocean: a century of decline. [en ligne]. 2011. [Consulté le 10 septembre 2025]. Disponible à l'adresse : https://digital.csic.es/handle/10261/46225

CLIMATEDATA.CA, s.d. Understanding Shared Socio-economic Pathways (SSPs). *ClimateData.ca* [en ligne]. s.d. [Consulté le 4 mars 2025]. Disponible à l'adresse : https://climatedata.ca/resource/understanding-shared-socio-economic-pathways-ssps/

DRENKARD, Elizabeth J, STOCK, Charles, ROSS, Andrew C, DIXON, Keith W, ADCROFT, Alistair, ALEXANDER, Michael, BALAJI, Venkatramani, BOGRAD, Steven J, BUTENSCHÖN, Momme, CHENG, Wei, CURCHITSER, Enrique, LORENZO, Emanuele Di, DUSSIN, Raphael, HAYNIE, Alan C, HARRISON, Matthew, HERMANN, Albert, HOLLOWED, Anne, HOLSMAN, Kirstin, HOLT, Jason, JACOX, Michael G, JANG, Chan Joo, KEARNEY, Kelly A, MUHLING, Barbara A, BUIL, Mercedes Pozo, SABA, Vincent, SANDØ, Anne Britt, TOMMASI, Désirée et WANG, Muyin, 2021. Next-generation regional ocean projections for living marine resource management in a changing climate. *ICES Journal of Marine Science*. 1 septembre 2021. Vol. 78, n° 6, pp. 1969-1987. DOI 10.1093/icesjms/fsab100.

DUNNE, J. P., HOROWITZ, L. W., ADCROFT, A. J., GINOUX, P., HELD, I. M., JOHN, J. G., KRASTING, J. P., MALYSHEV, S., NAIK, V., PAULOT, F., SHEVLIAKOVA, E., STOCK, C. A., ZADEH, N., BALAJI, V., BLANTON, C., DUNNE, K. A., DUPUIS, C., DURACHTA, J., DUSSIN, R., GAUTHIER, P. P. G., GRIFFIES, S. M., GUO, H., HALLBERG, R. W., HARRISON, M., HE, J., HURLIN, W., MCHUGH, C., MENZEL, R., MILLY, P. C. D., NIKONOV, S., PAYNTER, D. J., PLOSHAY, J., RADHAKRISHNAN, A., RAND, K., REICHL, B. G., ROBINSON, T., SCHWARZKOPF, D. M., SENTMAN, L. T., UNDERWOOD, S., VAHLENKAMP, H., WINTON, M., WITTENBERG, A. T., WYMAN, B., ZENG, Y. et ZHAO, M., 2020a. The GFDL Earth System Model Version 4.1 (GFDL-ESM 4.1): Overall Coupled Model Description and Simulation Characteristics. *Journal of Advances in Modeling Earth Systems*. novembre 2020. Vol. 12, n° 11, pp. e2019MS002015. DOI 10.1029/2019MS002015.

DUNNE, J. P., HOROWITZ, L. W., ADCROFT, A. J., GINOUX, P., HELD, I. M., JOHN, J. G., KRASTING, J. P., MALYSHEV, S., NAIK, V., PAULOT, F., SHEVLIAKOVA, E., STOCK, C. A., ZADEH, N., BALAJI, V., BLANTON, C., DUNNE, K. A., DUPUIS, C., DURACHTA, J., DUSSIN, R., GAUTHIER, P. P. G., GRIFFIES, S. M., GUO, H., HALLBERG, R. W., HARRISON, M., HE, J., HURLIN, W., MCHUGH, C., MENZEL, R., MILLY, P. C. D., NIKONOV, S., PAYNTER, D. J., PLOSHAY, J., RADHAKRISHNAN, A., RAND, K., REICHL, B. G., ROBINSON, T., SCHWARZKOPF, D. M., SENTMAN, L. T., UNDERWOOD, S., VAHLENKAMP, H., WINTON, M., WITTENBERG, A. T., WYMAN, B., ZENG, Y. et ZHAO, M., 2020b. The GFDL Earth System Model Version 4.1 (GFDL-ESM 4.1): Overall Coupled Model Description and Simulation Characteristics. *Journal of Advances in Modeling Earth Systems*. 2020. Vol. 12, n° 11, pp. e2019MS002015. DOI 10.1029/2019MS002015.

EYRING, Veronika, BONY, Sandrine, MEEHL, Gerald A., SENIOR, Catherine A., STEVENS, Bjorn, STOUFFER, Ronald J. et TAYLOR, Karl E., 2016. Overview of the Coupled Model Intercomparison Project Phase 6 (CMIP6) experimental design and organization. *Geoscientific Model Development*. 26 mai 2016. Vol. 9, n° 5, pp. 1937-1958. DOI 10.5194/gmd-9-1937-2016.

FOWLER, H. J., BLENKINSOP, S. et TEBALDI, C., 2007. Linking climate change modelling to impacts studies: recent advances in downscaling techniques for hydrological modelling. *International Journal of Climatology*. 2007. Vol. 27, n° 12, pp. 1547-1578. DOI 10.1002/joc.1556.

GUINOTTE, John M. et FABRY, Victoria J., 2008. Ocean Acidification and Its Potential Effects on Marine Ecosystems. *Annals of the New York Academy of Sciences*. 2008. Vol. 1134, n° 1, pp. 320-342. DOI 10.1196/annals.1439.013.

HASTINGS, Reuben A., RUTTERFORD, Louise A., FREER, Jennifer J., COLLINS, Rupert A., SIMPSON, Stephen D. et GENNER, Martin J., 2020. Climate Change Drives Poleward Increases and Equatorward Declines in Marine Species. *Current Biology*. 20 avril 2020. Vol. 30, n° 8, pp. 1572-1577.e2. DOI 10.1016/j.cub.2020.02.043.

HEENAN, Adel, POMEROY, Robert, BELL, Johann, MUNDAY, Philip L., CHEUNG, William, LOGAN, Cheryl, BRAINARD, Russell, YANG AMRI, Affendi, ALIÑO, Porfirio, ARMADA, Nygiel, DAVID, Laura, RIVERA-GUIEB, Rebecca, GREEN, Stuart, JOMPA, Jamaluddin, LEONARDO, Teresa, MAMAUAG, Samuel, PARKER, Britt, SHACKEROFF, Janna et YASIN, Zulfigar, 2015. A climate-informed, ecosystem approach to fisheries management. *Marine Policy*. 1 juillet 2015. Vol. 57, pp. 182-192. DOI 10.1016/j.marpol.2015.03.018.

HILDÉN, Mikael, JEUKEN, Ad et ZANDERSEN, Marianne, 2018. Storylines and Pathways for Adaptation in Europe. In : *Adapting to Climate Change in Europe* [en ligne]. Elsevier. pp. 7-47. [Consulté le 28 mars 2025]. ISBN 978-0-12-849887-3. Disponible à l'adresse : https://linkinghub.elsevier.com/retrieve/pii/B9780128498873000022

HOBDAY, Alistair J., SPILLMAN, Claire M., EVESON, J. Paige, HARTOG, Jason R., ZHANG, Xuebin et BRODIE, Stephanie, 2018. A Framework for Combining Seasonal Forecasts and Climate Projections to Aid Risk Management for Fisheries and Aquaculture. *Frontiers in Marine Science*. 23 avril 2018. Vol. 5, pp. 137. DOI 10.3389/fmars.2018.00137.

HOLLOWED, Anne Babcock, HOLSMAN, Kirstin K, WISE, Sarah P, HAYNIE, Alan C, CHENG, Wei, EVANS, Diana C K, HERMANN, Albert J, IANELLI, James N, KEARNEY, Kelly A, PUNT, Andre E, REUM, Jonathan C P, STRAM, Diana L et SZUWALSKI, Cody S, 2025. Development of climate informed management scenarios for fisheries in the eastern Bering Sea. *ICES Journal of Marine Science*. 1 janvier 2025. Vol. 82, n° 1, pp. fsae034. DOI 10.1093/icesjms/fsae034.

HUANG, Boyin, LIU, Chunying, BANZON, Viva, FREEMAN, Eric, GRAHAM, Garrett, HANKINS, Bill, SMITH, Tom et ZHANG, Huai-Min, 2021. Improvements of the Daily Optimum Interpolation Sea Surface Temperature (DOISST) Version 2.1. [en ligne]. 2021. [Consulté le 28 août 2025]. Disponible à l'adresse : https://repository.library.noaa.gov/view/noaa/33412

JOHANSEN, Jacob L., MITCHELL, Matthew D., VAUGHAN, Grace O., RIPLEY, Daniel M., SHIELS, Holly A. et BURT, John A., 2024. Impacts of ocean warming on fish size reductions on the world's hottest coral reefs. *Nature Communications*. 1 juillet 2024. Vol. 15, n° 1, pp. 5457. DOI 10.1038/s41467-024-49459-8.

KRISTIANSEN, Trond, BUTENSCHÖN, Momme et PECK, Myron A., 2024. Statistically downscaled CMIP6 ocean variables for European waters. *Scientific Reports*. 12 janvier 2024. Vol. 14, n° 1, pp. 1209. DOI 10.1038/s41598-024-51160-1.

LAL, Murari, MCGREGOR, John L. et NGUYEN, Kim C., 2008. Very high-resolution climate simulation over Fiji using a global variable-resolution model. *Climate Dynamics*. 1 février 2008. Vol. 30, n° 2, pp. 293-305. DOI 10.1007/s00382-007-0287-0.

LINDMARK, Max, AUDZIJONYTE, Asta, BLANCHARD, Julia L. et GÅRDMARK, Anna, 2022. Temperature impacts on fish physiology and resource abundance lead to faster growth but smaller fish sizes and yields under warming. *Global Change Biology*. novembre 2022. Vol. 28, n° 21, pp. 6239-6253. DOI 10.1111/gcb.16341.

OEDEKOVEN, Cornelia S, THOMAS, Len, HARRIS, Catriona M, SCOTT-HAYWARD, Lindesay A S, HARRIS, Danielle, CHUDSKINSKA, Magda, PAXTON, Charles G M, BERGER, Alba Solsona et BAUMANN-PICKERING, Simone, 2023. Methods comparison for analysing PAM data to detect a change in cue detection rate of cetaceans related to a potential disturbance. . 2023.

OLIVEROS-RAMOS, Ricardo, SHIN, Yunne-Jai, GUTIERREZ, Dimitri et TRENKEL, Verena M, 2025. Multi-model approach for statistical downscaling and bias correction of Earth system model outputs for marine ecosystem impact applications. *ICES Journal of Marine Science*. 1 juin 2025. Vol. 82, n° 6, pp. fsaf073. DOI 10.1093/icesjms/fsaf073.

POZO BUIL, Mercedes, FIECHTER, Jerome, JACOX, Michael G., BOGRAD, Steven J. et ALEXANDER, Michael A., 2023. Evaluation of Different Bias Correction Methods for Dynamical Downscaled Future Projections of the California Current Upwelling System. *Earth and Space Science*. 2023. Vol. 10, n° 12, pp. e2023EA003121. DOI 10.1029/2023EA003121.

RIAHI, Keywan, VAN VUUREN, Detlef P., KRIEGLER, Elmar, EDMONDS, Jae, O'NEILL, Brian C., FUJIMORI, Shinichiro, BAUER, Nico, CALVIN, Katherine, DELLINK, Rob, FRICKO, Oliver, LUTZ, Wolfgang, POPP, Alexander, CUARESMA, Jesus Crespo, KC, Samir, LEIMBACH, Marian, JIANG, Leiwen, KRAM, Tom, RAO, Shilpa, EMMERLING, Johannes, EBI, Kristie, HASEGAWA, Tomoko, HAVLIK, Petr, HUMPENÖDER, Florian, DA SILVA, Lara Aleluia, SMITH, Steve, STEHFEST, Elke, BOSETTI, Valentina, EOM, Jiyong, GERNAAT, David, MASUI, Toshihiko, ROGELJ, Joeri, STREFLER, Jessica, DROUET, Laurent, KREY, Volker, LUDERER, Gunnar, HARMSEN, Mathijs, TAKAHASHI, Kiyoshi, BAUMSTARK, Lavinia, DOELMAN, Jonathan C., KAINUMA, Mikiko, KLIMONT, Zbigniew, MARANGONI, Giacomo, LOTZE-CAMPEN, Hermann, OBERSTEINER, Michael, TABEAU, Andrzej et TAVONI, Massimo, 2017a. The Shared Socioeconomic Pathways and their energy, land use, and greenhouse gas emissions implications: An overview. *Global Environmental Change*. 1 janvier 2017. Vol. 42, pp. 153-168. DOI 10.1016/j.gloenvcha.2016.05.009.

RIAHI, Keywan, VAN VUUREN, Detlef P, KRIEGLER, Elmar et O'NEILL, Brian, 2017b. The Shared Socio-Economic Pathways (SSPs): An Overview. . 2017.

RUTI, P. M., SOMOT, S., GIORGI, F., DUBOIS, C., FLAOUNAS, E., OBERMANN, A., DELL'AQUILA, A., PISACANE, G., HARZALLAH, A., LOMBARDI, E., AHRENS, B., AKHTAR, N., ALIAS, A., ARSOUZE, T., AZNAR, R., BASTIN, S., BARTHOLY, J., BÉRANGER, K., BEUVIER, J., BOUFFIES-CLOCHÉ, S., BRAUCH, J., CABOS, W., CALMANTI, S., CALVET, J.-C., CARILLO, A., CONTE, D., COPPOLA, E., DJURDJEVIC, V., DROBINSKI, P., ELIZALDE-ARELLANO, A., GAERTNER, M., GALÀN, P., GALLARDO, C., GUALDI, S., GONCALVES, M., JORBA, O., JORDÀ, G., L'HEVEDER, B., LEBEAUPIN-BROSSIER, C., LI, L., LIGUORI, G., LIONELLO, P., MACIÀS, D., NABAT, P., ÖNOL, B., RAIKOVIC, B., RAMAGE, K., SEVAULT, F., SANNINO, G., STRUGLIA, M. V., SANNA, A., TORMA, C. et VERVATIS, V., 2016. Med-CORDEX Initiative for Mediterranean Climate Studies. *Bulletin of the American Meteorological Society*. 1 juillet 2016. Vol. 97, n° 7, pp. 1187-1208. DOI 10.1175/BAMS-D-14-00176.1.

SCHNASE, John L., LEE, Tsengdar J., MATTMANN, Chris A., LYNNES, Christopher S., CINQUINI, Luca, RAMIREZ, Paul M., HART, Andrew F., WILLIAMS, Dean N., WALISER, Duane, RINSLAND, Pamela, WEBSTER, W. Phillip, DUFFY, Daniel Q., MCINERNEY, Mark A., TAMKIN, Glenn S., POTTER, Gerald L. et CARRIERE, Laura, 2016. Big Data Challenges in Climate Science: Improving the next-generation cyberinfrastructure. *IEEE Geoscience and Remote Sensing Magazine*. septembre 2016. Vol. 4, n° 3, pp. 10-22. DOI 10.1109/MGRS.2015.2514192.

SPRFMO, [sans date]. Convention Area » SPRFMO. [en ligne]. [Consulté le 28 août 2025]. Disponible à l'adresse : https://www.sprfmo.int/about/convention-area

STOKLOSA, Jakub, DALY, Christopher, FOSTER, Scott D., ASHCROFT, Michael B. et WARTON, David I., 2015. A climate of uncertainty: accounting for error in climate variables for species distribution models. *Methods in Ecology and Evolution*. 2015. Vol. 6, n° 4, pp. 412-423. DOI 10.1111/2041-210X.12217.

TEUTSCHBEIN, Claudia et SEIBERT, Jan, 2012. Bias correction of regional climate model simulations for hydrological climate-change impact studies: Review and evaluation of different methods. *Journal of Hydrology*. 16 août 2012. Vol. 456-457, pp. 12-29. DOI 10.1016/j.jhydrol.2012.05.052.

TITTENSOR, Derek P., NOVAGLIO, Camilla, HARRISON, Cheryl S., HENEGHAN, Ryan F., BARRIER, Nicolas, BIANCHI, Daniele, BOPP, Laurent, BRYNDUM-BUCHHOLZ, Andrea, BRITTEN, Gregory L., BÜCHNER, Matthias, CHEUNG, William W. L., CHRISTENSEN, Villy, COLL, Marta, DUNNE, John P., EDDY, Tyler D., EVERETT, Jason D., FERNANDES-SALVADOR, Jose A., FULTON, Elizabeth A., GALBRAITH, Eric D., GASCUEL, Didier, GUIET, Jerome, JOHN, Jasmin G., LINK, Jason S., LOTZE, Heike K., MAURY, Olivier, ORTEGA-CISNEROS, Kelly, PALACIOS-ABRANTES, Juliano, PETRIK, Colleen M., DU PONTAVICE, Hubert, RAULT, Jonathan, RICHARDSON, Anthony J., SHANNON, Lynne, SHIN, Yunne-Jai, STEENBEEK, Jeroen, STOCK, Charles A. et BLANCHARD, Julia L., 2021. Next-generation ensemble projections reveal higher climate risks for marine ecosystems. *Nature Climate Change*. novembre 2021. Vol. 11, n° 11, pp. 973-981. DOI 10.1038/s41558-021-01173-9.

VAN VUUREN, Detlef P., STEHFEST, Elke, DEN ELZEN, Michel G. J., KRAM, Tom, VAN VLIET, Jasper, DEETMAN, Sebastiaan, ISAAC, Morna, KLEIN GOLDEWIJK, Kees, HOF, Andries, MENDOZA BELTRAN, Angelica, OOSTENRIJK, Rineke et VAN RUIJVEN, Bas, 2011. RCP2.6: exploring the possibility to keep global mean temperature increase below 2°C. *Climatic Change*. novembre 2011. Vol. 109, n° 1-2, pp. 95-116. DOI 10.1007/s10584-011-0152-3.

VOGEL, Jacqueline M., LONGO, Catherine, SPIJKERS, Jessica, PALACIOS-ABRANTES, Juliano, MASON, Julia, WABNITZ, Colette C. C., CHEUNG, William, SUMAILA, U. Rashid, MUNRO, Gordon, GLASER, Sarah, BELL, Johann, TIAN, Yongjun, SHACKELL, Nancy L., SELIG, Elizabeth R., LE BILLON, Philippe, WATSON, James R., HENDRIX, Cullen, PINSKY, Malin L., VAN PUTTEN, Ingrid, KARR, Kendra, PAPAIOANNOU, Eva A. et FUJITA, Rod, 2023. Drivers of conflict and resilience in shifting transboundary fisheries. *Marine Policy*. 1 septembre 2023. Vol. 155, pp. 105740. DOI 10.1016/j.marpol.2023.105740.

XU, Zhongfeng, HAN, Ying et YANG, Zongliang, 2019. Dynamical downscaling of regional climate: A review of methods and limitations. *Science China Earth Sciences*. février 2019. Vol. 62, n° 2, pp. 365-375. DOI 10.1007/s11430-018-9261-5.

Appendices

Appendix I. Effect of climate change on fish stocks/niche

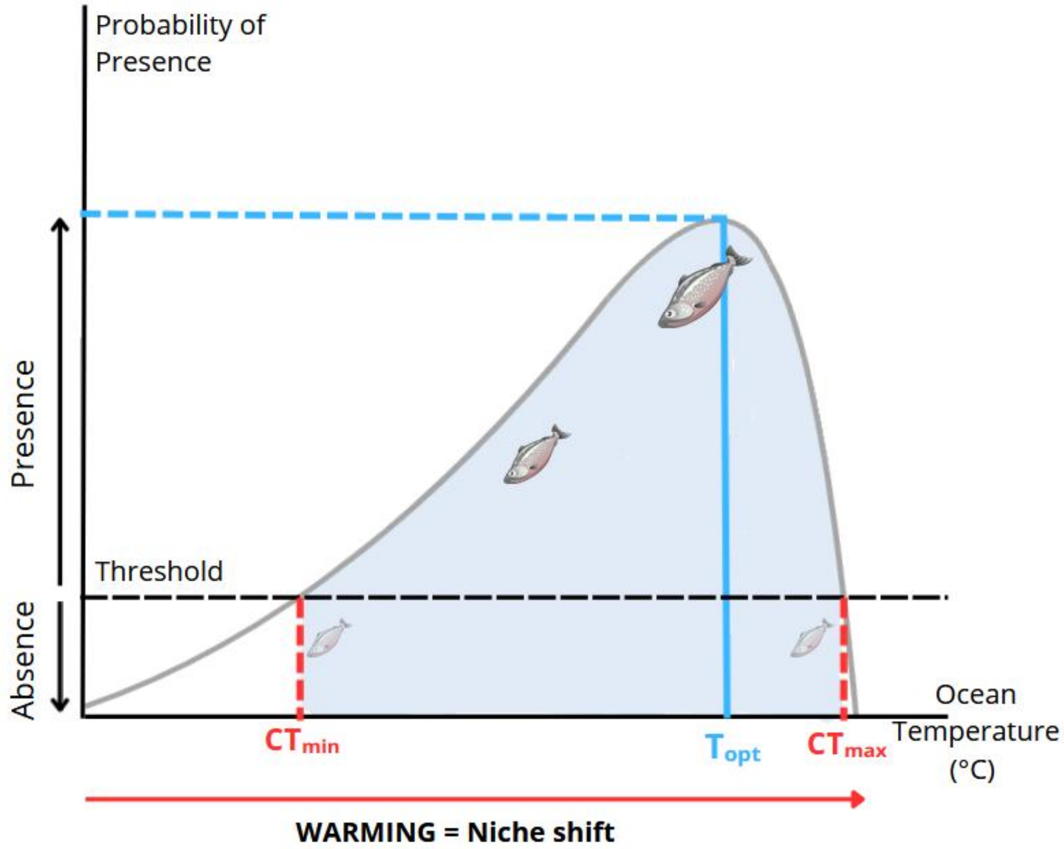

Appendix II. Information about SSP scenarios

Figure A1. Typology of Shared Socioeconomic Pathways (SSPs) plotted by socio-economic challenges for mitigation (y-axis) and adaptation (x-axis). (Riahi *et al.*, 2017b)

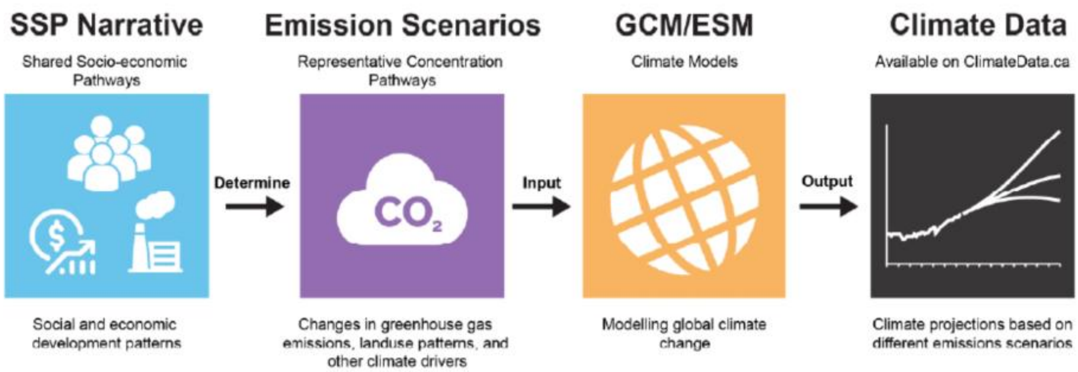

Figure A2. Simplified workflow from SSP narratives through emissions scenarios and Earth System Models (ESMs) to climate output data. (ClimateData.ca, s.d)

Appendix III. Area of application of the SPRFMO Convention (SPRFMO, s.d)

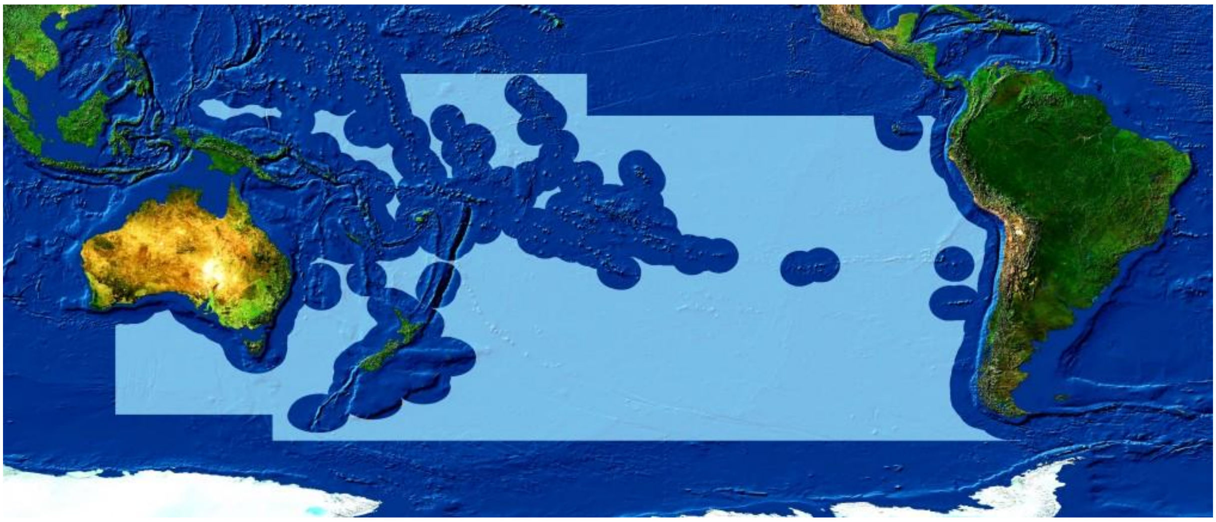

Appendix IV. Estimated cost of Cross-Validation

Scenario	Folds (k)	Total fitted models	Prediction bundles per model	Size per bundle (4 ESMs)	Total prediction storage
No CV (all 30 models)	1	30	1	150 GB	**1,500 GB (1.5 TB)**
6-fold CV (all models)	6	180	1 per fold	150 GB	**9,000 GB (9.0 TB)**
12-fold CV (all models)	12	360	1 per fold	150 GB	**18,000 GB (18.0 TB)**

Note. The totals shown reflect prediction files only (historical + future per ESM). They exclude fitted model objects (~1 GB each), cross-validation diagnostics, logs, intermediate tiles/chunks, and the input databases themselves. In practice, end-to-end storage would therefore be substantially larger than the figures reported here.

Appendix V. Complete table of indicators (A) + regional subset maps (B + C)

Indicator	Range	Description
A. FUTURE INDICATORS		
Indicators A type		
A1: overlap	[0, 1]	Overlap of the range between future and present bias
A2 : pmax	$\mathbb{R}$	Number of values outside the range (max SST)
A3 : pmin	$\mathbb{R}$	Number of values outside the range (min SST)
A4 : cte_max	$\mathbb{R}$	Average value outside of range (max SST)
A5 : cte_min	$\mathbb{R}$	Average value outside of range (min SST)
A6 : omax	$\mathbb{R}$	Same as A4 but taking worst value
A7 : omin	$\mathbb{R}$	Same as A5 but taking worst value
Subsets of indicator A		
A1-A7	For all quantiles	
A8–A14	For quantiles 0.5 and below	
A15-A21	For quantiles 9.5 and above	
A22-A29	For El Niño3.4	
A30-35	For El Niño1+2	
B. RESIDUAL INDICATORS		
Present error Indicators		
B1	$[0, \infty)$	Mean absolute error (MAE) between predicted and observed SST across the full domain. Measures overall fit.
B2	$\mathbb{R}^+$	Range of residuals (max – min) across the full domain.
B3	[-1, 1]	Mean sign of residuals, indicating global bias asymmetry (over- vs underestimation).
B4	$\mathbb{R}$	Conditional Tail Expectation (CTE) between Q95 and Q05.
B5	$\mathbb{R}$	CTE between maximum and minimum residuals.
B6	$[0, \infty)$	MAE of Q05.

B7	[0, ∞)	MAE of Q95.
Residuals and biases in Niño regions		
B8	[0, ∞)	MAE in Niño3.4 region.
B9	[0, ∞)	MAE in Niño1+2 region.
B10	ℝ	Residual asymmetry (mean positive – mean negative residuals) across the full domain.
B11	ℝ	Residual asymmetry in Niño3.4 region 5mean pos – mean neg)..
B12	ℝ	Residual asymmetry in Niño1+2 5region mean pos – mean neg)..
B13	ℝ	Mean bias in hot extremes (min) in Niño3.4 (present).
B14	ℝ	Mean bias in cold extremes (max) in Niño3.4 (present).
B15	ℝ	Mean bias in hot extremes (min) in Niño1+2 (present).
B16	ℝ	Mean bias in cold extremes (max) in Niño1+2 (present).
C. EXPLAINED DEVIANCE		
C1	[0,1]	Deviance explained, full dataset.
C2	[0,1]	Deviance explained, coldest pixels.
C3	[0,1]	Deviance explained, warmest pixels.
C4	[0,1]	Deviance explained, shelf regions.
C5	[0,1]	Deviance explained, open ocean.
C6	[0,1]	Deviance explained, shallow waters.
C7	[0,1]	Deviance explained, deep waters.
C8	[0,1]	Deviance explained, Niño3.4.
C9	[0,1]	Deviance explained, Niño1+2.
C10	[0,1]	Deviance explained, outside Niño3.4.
C11	[0,1]	Deviance explained, outside Niño1+2.
C12	[0,1]	Regional deviance: Australia.
C13	[0,1]	Regional deviance: South America.

A : Complete table of Indicators

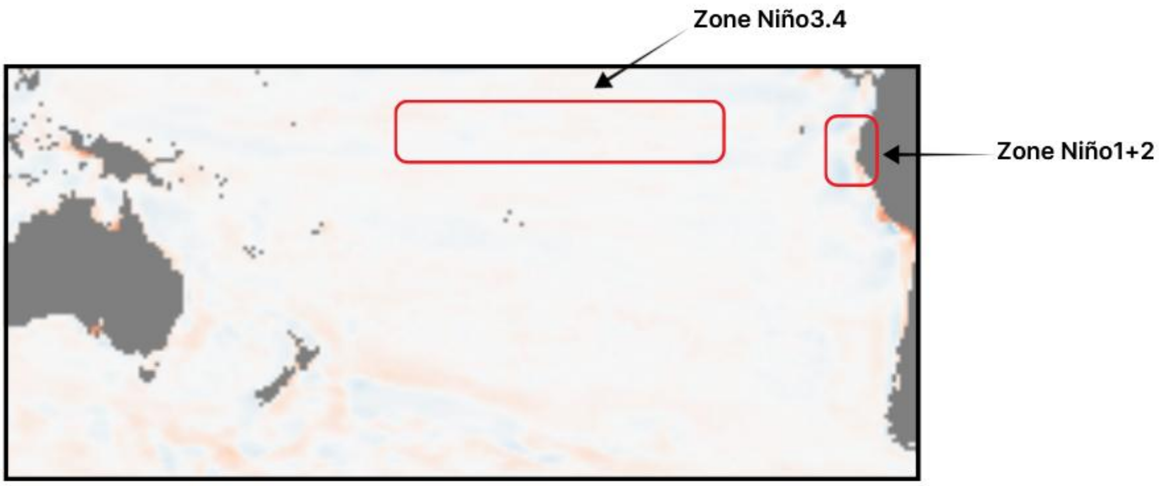

B : El Niño zones (for indicators subsets)

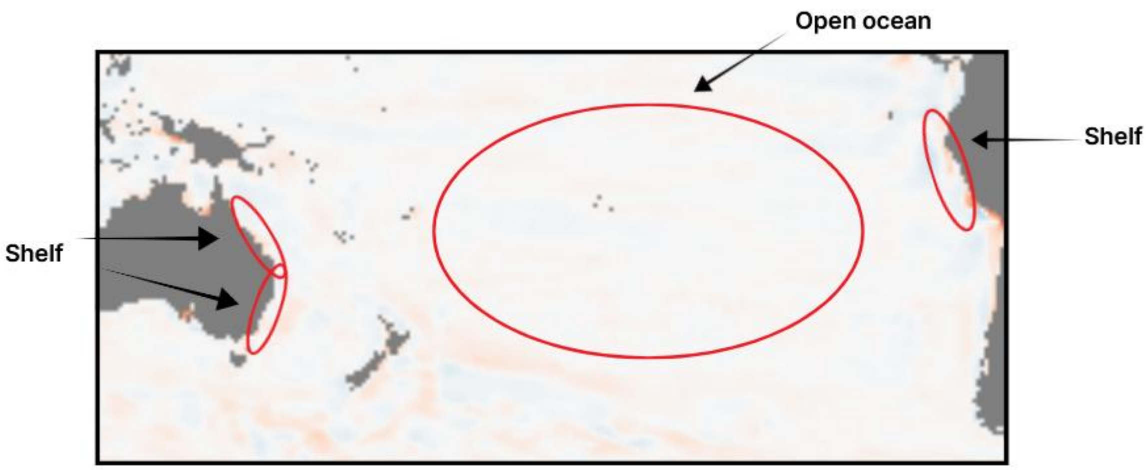

C : Open Ocean vs shelf zones (for indicators subsets)

Appendix VI. Heatmaps for IPSL ESM (CMIP5 and CMIP6)

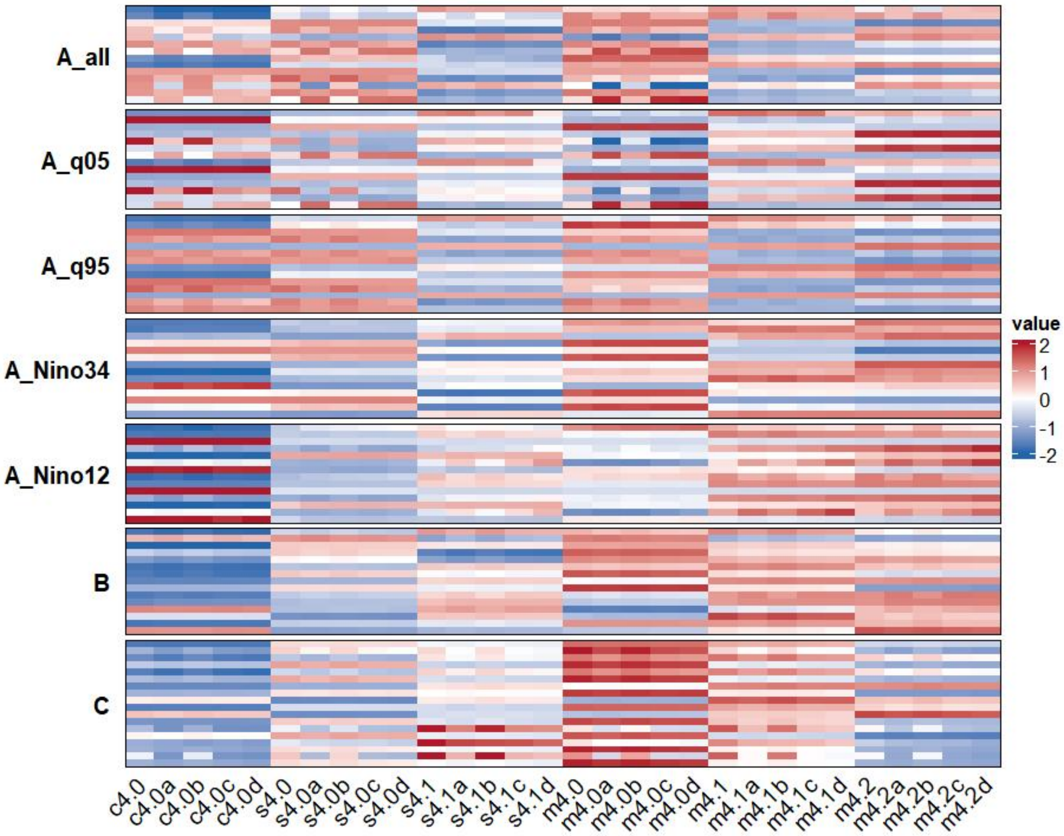

Figure A. Heatmap of indicators for GFDL CMIP6 Earth System Model

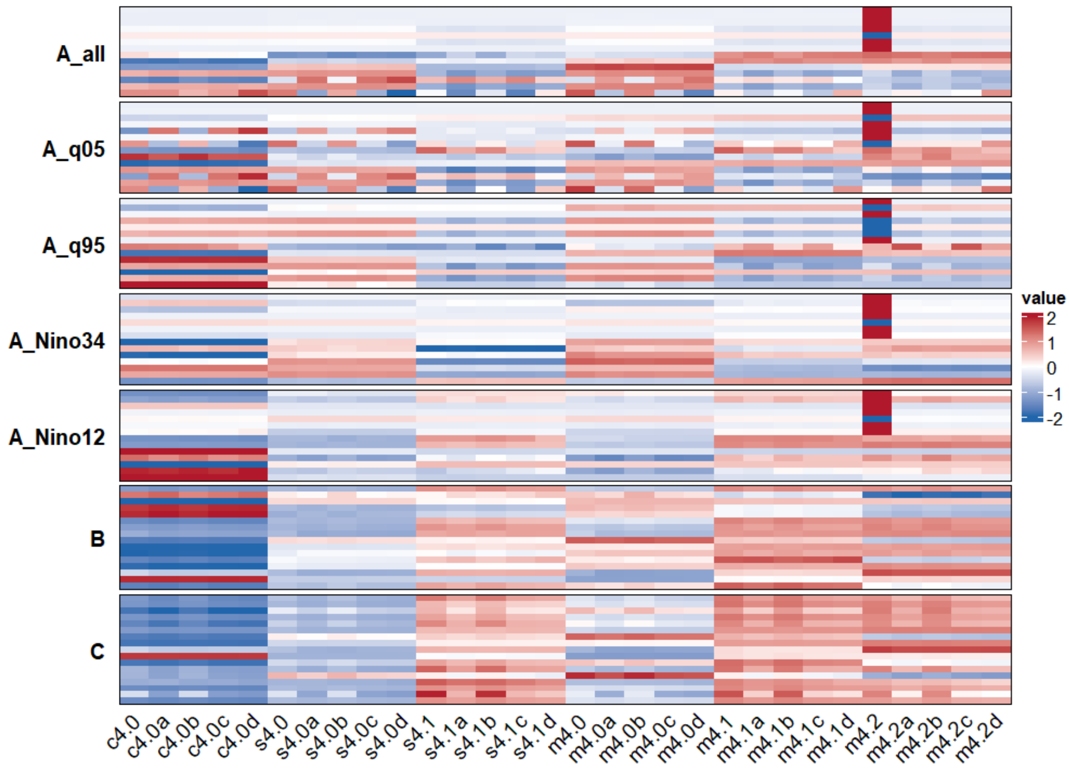

Figure B. Heatmap of indicators for GFDL CMIP6 Earth System Model

Appendix VII. Time-series for model c4.0c for all ESM and CMIP variations + overshoot scenario (IPSL CMIP6)

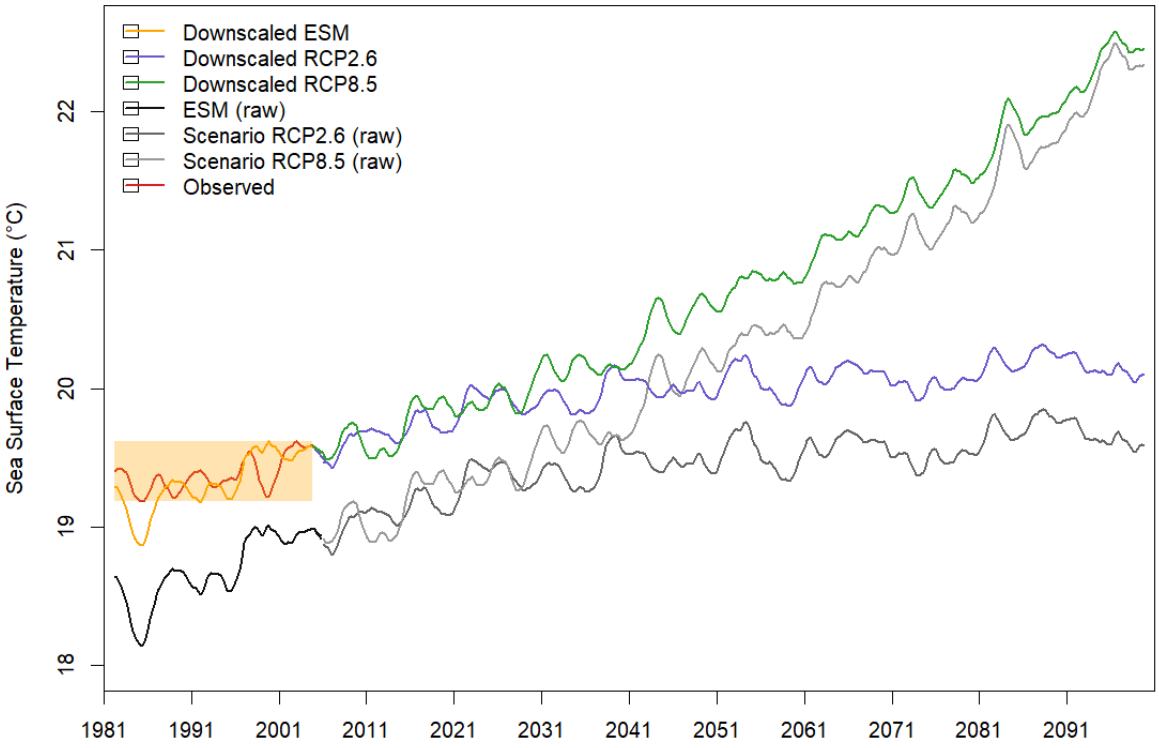

Figure A. Time-series for IPSL CMIP5 ESM (historical + future scenario) raw and downscaled projections.

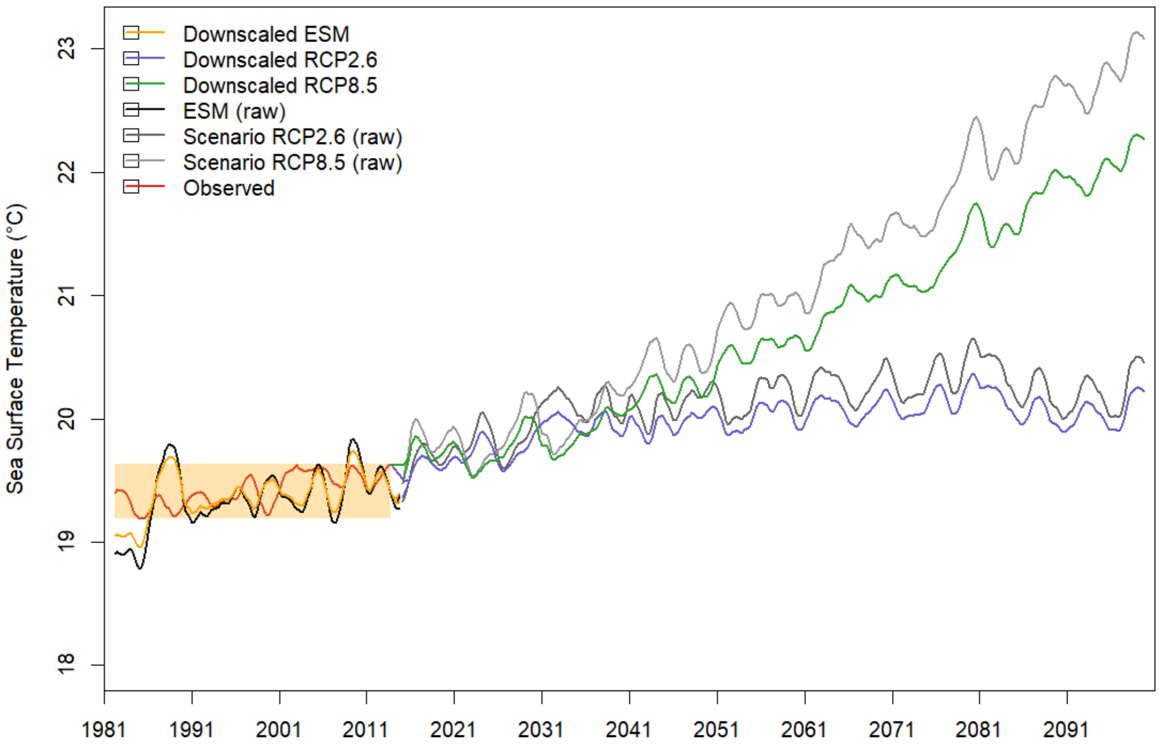

Figure B. Time-series for IPSL CMIP6 ESM (historical + future scenario) raw and downscaled projections.

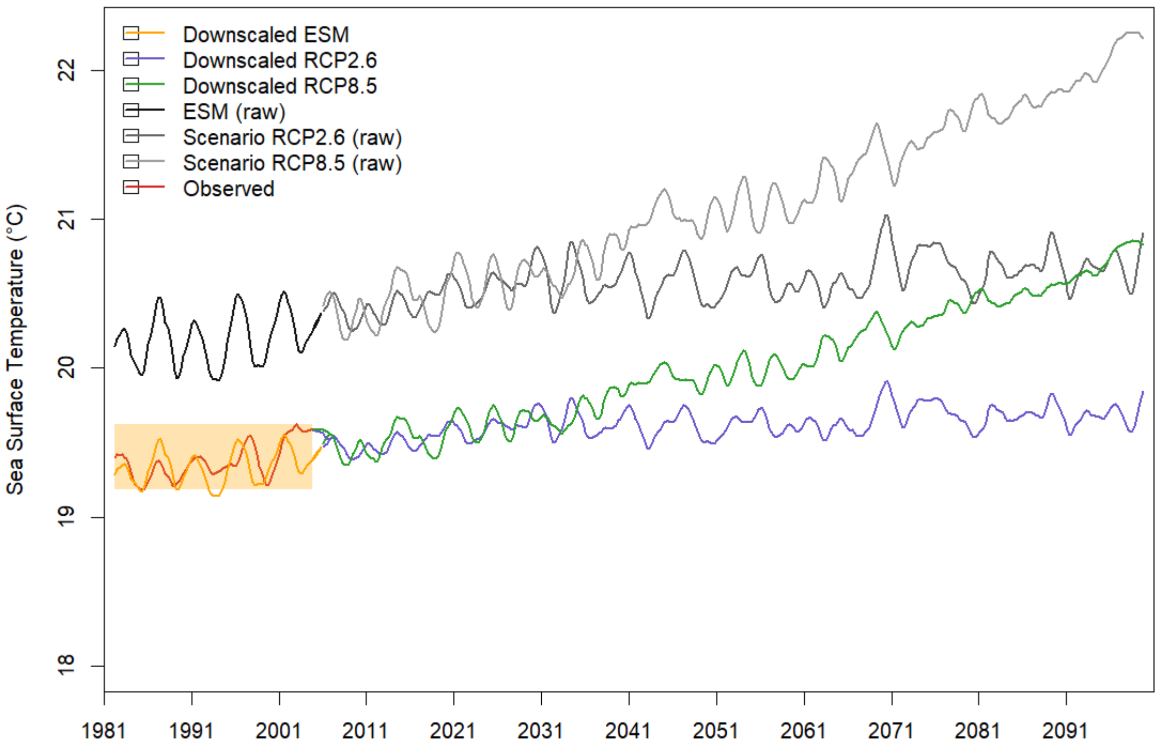

Figure C. Time-series for GFDL CMIP5 ESM (historical + future scenario) raw and downscaled projections.

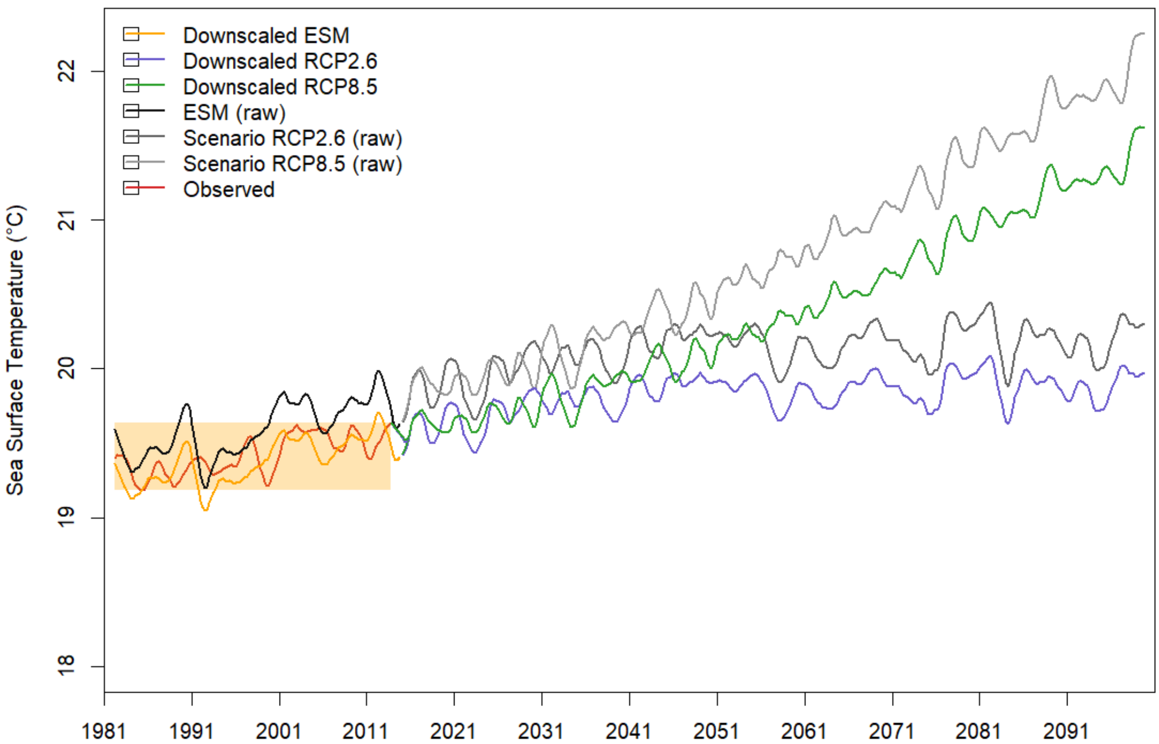

Figure D. Time-series for GFDL CMIP6 ESM (historical + future scenario) raw and downscaled projections.

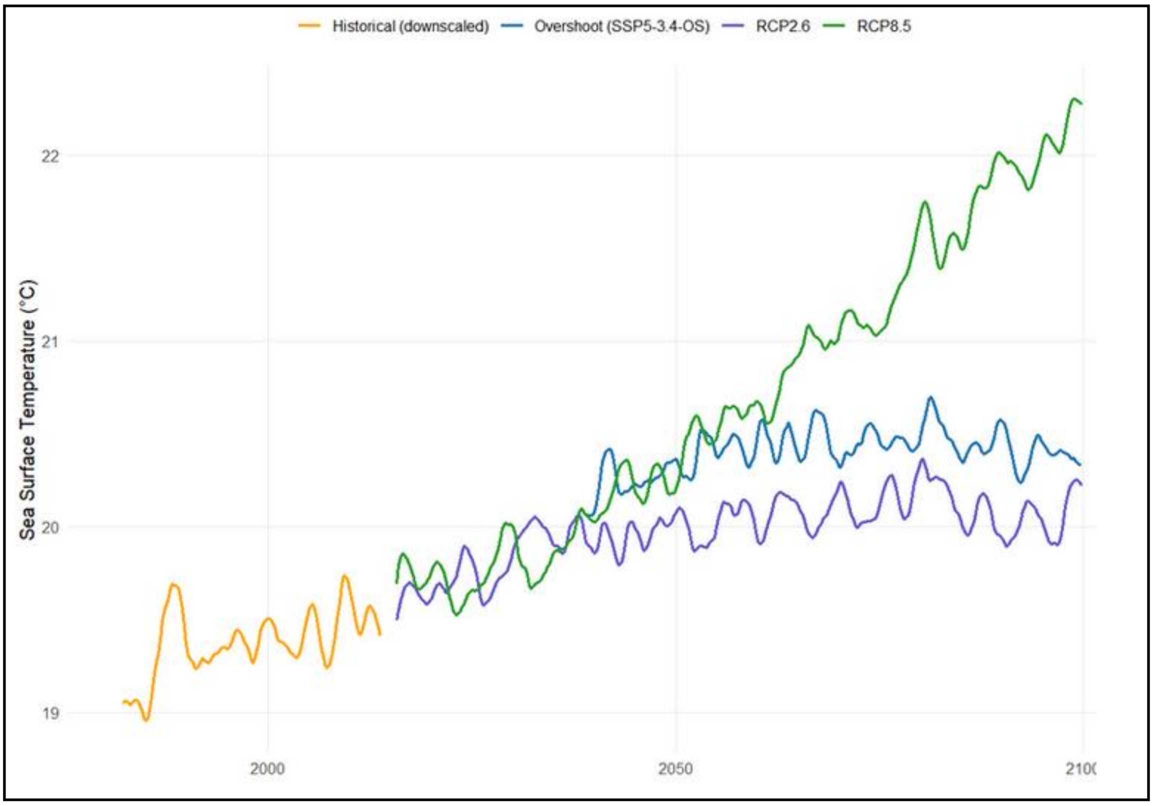

Figure E. Time-series for IPSL CMIP6 ESM (historical + future scenario + overshoot) downscaled projections.

Appendix VIII. Technical Strategies for Large-Domain Statistcal Downscaling

Strategy	Description	Why It Was Needed	Benefit / Performance Gain
Memory-efficient processing	Removed intermediates (*rm(), gc()*), used chunked loading.	Full South Pacific datasets saturated RAM.	Prevented crashes, allowed runs to finish.
Parallelized *GAM/BAM* fitting	Used *bam()* with *nthreads=4*, 24 cores per run; *gam()* only for null model.	Seasonal/monthly models otherwise required several days.	Reduced runtime to a few hours.
Model object compression	Custom *compact_gam()* stripped environments and fitted values.	Default GAM objects >1 GB each.	5–10× smaller files, feasible storage.
Switch from *CSV* to *Parquet*	Stored data in compressed, columnar *Parquet* format.	*CSV* files were too large/slow to reload repeatedly.	3–6× smaller, 2–5× faster I/O, selective loading.
Modular and reproducible workflow	Standardized naming, split scripts by step, consistent covariates.	Lots of models × datasets made tracking outputs messy.	Improved traceability and comparison.
Avoiding *tidyverse/dplyr*	Replaced with data.table or base R for joins/filtering.	*dplyr was slower, high RAM use for multi-GB SST data.*	Faster execution, lower memory footprint.

Appendix IX. Possible delimitation for smaller and more regional models proposed by a fellow intern project.

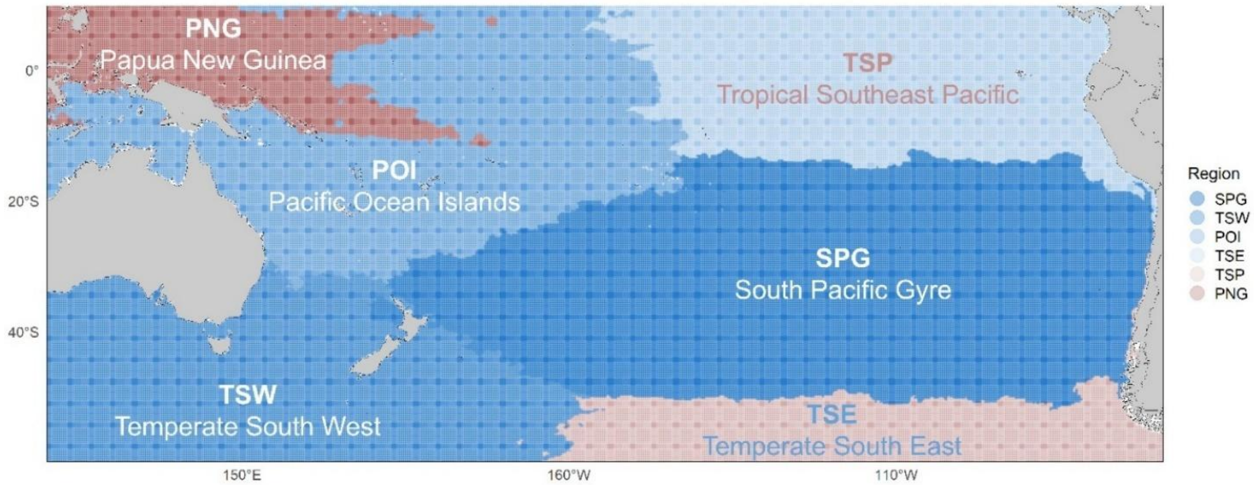

Quatrième de couverture

	Diplôme : Ingénieur agronome Spécialité : Sciences halieutiques et aquacoles Spécialisation / option : « Statistiques et modélisation » Enseignant référent : Etienne RIVOT
Auteur(s) : Lou BEATA Date de naissance* : 20/02/2002	Organisme d'accueil : MARBEC Adresse :
Nb pages : 33 Annexe(s) : IX	
Année de soutenance : 2025	Maître de stage : Ricardo Oliveros-Ramos

Titre français : Projections haute résolution de la température de surface de la mer dans le Pacifique Sud par descente d'échelle statistique et correction de biais.

Titre anglais : High-Resolution Projections of South Pacific Sea Surface Temperature through Statistical Downscaling and Bias Correction

Résumé :

Nous avons développé un cadre de descente d'échelle statistique et de correction de biais, adapté des travaux de Oliveros-Ramos et al. (2025), afin de transformer les sorties de température de surface de la mer (SST) issues des Earth System Models (ESMs), disponibles en basse résolution, en projections régionales haute résolution (0,25° × 0,25°) pour le Pacifique Sud. La méthodologie combine le quantile mapping, la modélisation spatio-temporelle à l'aide de Modèles Additifs Généralisés (GAMs), et la validation-croisée, en intégrant des covariables environnementales ainsi que des prédicteurs saisonniers pour améliorer la précision. Les sorties des ESMs ont été évaluées par rapport au jeu de données observationnel Optimum Interpolation SST (OI-SST), couvrant les périodes historique et future dans le cadre des ensembles CMIP5 et CMIP6, et sous différents scénarios de type Representative Concentration Pathways (RCPs) et Shared Socioeconomic Pathways (SSPs).

La performance des modèles a été évaluée à l'aide d'indicateurs adaptés, mesurant la persistance des biais, la structure des résidus et la déviance expliquée dans les climats présent et futur. Les résultats mettent en évidence l'influence des structures temporelles (constante, saisonnière, mensuelle) et de la complexité des covariables sur la robustesse des modèles, tout en révélant des différences entre générations successives de CMIP dans la reproduction de la variabilité de la SST dans le Pacifique Sud. Le cadre proposé a permis d'identifier les stratégies de correction de biais les plus efficaces à l'échelle subrégionale, produisant des projections SST corrigées et à haute résolution. Ces produits constituent des entrées environnementales essentielles pour les applications écologiques et halieutiques, permettant une prise de décision spatialisée et informée par le climat dans un contexte de réchauffement et de variabilité océaniques.

Abstract :

We developed a statistical downscaling and bias correction framework, adapted from Oliveros-Ramos et al. (2025), to transform coarse-resolution sea surface temperature (SST) outputs from Earth System Models (ESMs) into high-resolution (0.25° × 0.25°) regional projections for the South Pacific Ocean. The methodology combined quantile mapping, spatiotemporal modelling with Generalized Additive Models (GAMs), and cross-validation, incorporating environmental covariates and seasonal predictors to enhance accuracy. ESM outputs were evaluated against the Optimum Interpolation SST (OI-SST) observational dataset, covering both historical and future periods from CMIP5 and CMIP6 ensembles under Representative Concentration Pathways (RCPs) and Shared Socioeconomic Pathways (SSPs).

Model performance was assessed using tailored indicators of bias persistence, residual structure, and explained deviance across present and future climates. Results highlight how temporal structures (constant, seasonal, monthly) and covariate complexity influence model robustness, while also revealing differences between successive CMIP generations in reproducing South Pacific SST variability. The framework identified the most effective bias correction strategies across subregional scales, producing high-resolution, bias-corrected SST projections. These products provide critical environmental inputs for ecological and fisheries applications, enabling spatially targeted and climate-informed decision-making in the context of ongoing ocean warming and variability.

Mots clés :
descente d’échelle statistique; correction de biais; SST; CMIP5; CMIP6; scenario; changement climatique ; pêcheries

Key words :
statistical downscaling; bias correction; SST; CMIP5; CMIP6; scenario; climate change; fisheries